Cranial Synchondroses of Primates at Birth

Timothy D. Smith[1], Rebecca L. Reynolds[2], Nanami Mano[1], Brody J. Wood[1], Lanre Oladipupo[1], Gabriel K. Hughes[1], Haley M. Corbin[2], Jane Taylor[3], Alexander Ufelle[4], Anne M. Burrows[5], Emily Durham[6], Christopher J. Vinyard[7], James J. Cray[3,8], Valerie B. DeLeon[9]

1, School of Physical Therapy, Slippery Rock University, Slippery Rock, PA 16057; 2, Department of Public Health and Social Work, Slippery Rock University; 3, Department of Biomedical Education and Anatomy, The Ohio State College of Medicine, Columbus, OH 43210; 4, Department of Public Health and Social Work, Slippery Rock University, Slippery Rock, PA 16057; 5, Department of Physical Therapy, Duquesne University, Pittsburgh, PA 15282; 6, Department of Anthropology, Penn State University, State College, PA 16801; 7, Department of Anatomy and Neurobiology, Northeast Ohio Medical University, Rootstown, OH 44272; 8, Division of Biosciences, The Ohio State College of Dentistry, Columbus OH 43210; 9, Department of Anthropology, University of Florida, Gainesville, FL 32611.

Funding: NSF; grant numbers BCS-1830894, BCS-1830919, BCS-1231717, BCS-1231350, BCS-1728263.

Correspondence to:

Address: Tim D. Smith, Ph.D.

School of Physical Therapy

Slippery Rock University

Slippery Rock, PA 16057

E-mail: timothy.smith@sru.edu

ABSTRACT

Cranial synchondroses are cartilaginous joints between basicranial bones or between basicranial bones and septal cartilage, and have been implicated as having a potential active role in determining craniofacial form. However, few studies have examined them histologically. Using histological and immunohistochemical methods, we examined all basicranial joints in serial sagittal sections of newborn heads from nine genera of primates (five anthropoids, four strepsirrhines). Each synchondrosis was examined for characteristics of active growth centers, including a zonal distribution of proliferating and hypertrophic chondrocytes, as well as corresponding changes in matrix characteristics (i.e., density and organization of type II collagen). Results reveal three midline and three bilateral synchondroses possess attributes of active growth centers in all species (sphenooccipital, intrasphenoidal, presphenoseptal). One midline synchondrosis (ethmoseptal) and one bilateral synchondrosis (alibasisphenoidal, ABS) are active growth centers in some but not all newborn primates. ABS is oriented more anteriorly in monkeys compared to lemurs and bushbabies. The sphenoethmoidal synchondrosis (SES) varies at birth: in monkeys, it is a suture-like joint (i.e., fibrous tissue between the two bones); however, in strepsirrhines, the jugum sphenoidale is ossified while the mesethmoid remains cartilaginous. No species possesses a SES that has the organization of a growth plate. Overall, our findings demonstrate that only four midline synchondroses have the potential to actively affect basicranial angularity and facial orientation during the perinatal timeframe, while the SES of anthropoids essentially transitions toward a “suture-like” function, permitting passive growth postnatally. Loss of cartilaginous continuity at SES and reorientation of ABS distinguish monkeys from strepsirrhines.

Key Words: Craniofacial; Chondrocranium; Development; Perinatal

INTRODUCTION

Changes in the human cranial base have been well documented across prenatal and postnatal ontogeny (Ford, 1958; Baume, 1968; Enlow, 1976; Kjaer, 1990; Jeffery and Spoor, 2002). Within this context the brain is posited and been shown to drive much of the form of the calvarium. However, the dominant role of the brain in shaping the skull does not rule out other contributing factors. Synchondroses of the skull, cartilaginous joints, are distributed throughout the basicranium and facilitate increasing dimensions of the skull as a whole. Synchondroses with a zonal organization of chondrocytes into resting, proliferating, and hypertrophic zones are considered with "tissue separating power" (Baume, 1968, p 509), and are referred to as *growth centers*. Experimental evidence supports the intrinsic ability of synchondroses to actively propel ossification centers apart (Rönning and Kylämarkula, 1982; Hall and Precious, 2013; and see Hall, 2015), distinguishing them from sutures, which are considered passive *growth sites*. However, it is presently difficult to parse out the degree to which intrinsic factors such as synchondroses versus soft tissue matrices, such as the brain, have a stronger influence on basicranial form, or to what extent they have shared roles.

The mechanism by which the basicranium changes during ontogeny is not trivial and has implications bearing on development and evolution. This is especially true for the topic of basicranial angulation. During prenatal development, the human cranial base becomes more acutely angular (flexes) early, and to some degree becomes more obtusely angular (extends) during later fetal ontogeny (Jeffery and Spoor, 2002; Jeffery, 2005). Postnatally, the cranial base flexes again during early childhood, and then remains stable from approximately 4 years onward (Lieberman and McCarthy, 1999). During a similar postnatal sequence (according to dental stages), the chimpanzee cranial base gradually extends, and it has been suggested the same may be true of other Old World anthropoids (e.g., Sirianni and Van Ness, 1978). Further, acute angulation has been related to the retraction of the midface and orbits beneath the anterior cranial base in anthropoid primates (Lieberman et al., 2000; McBratney-Owen and Lieberman, 2003), although the midface may project forward to a varying degree. The close developmental link of the cranial base and midface is likely made by the nasal septal cartilage, which is continuous with the middle cranial base at the presphenoid. However, other authors have emphasized a close relationship exists between facial form and lateral regions of the basicranium (Bastir and Rosas, 2006; Neaux et al., 2013).

To date, broad interspecific comparisons of basicranial angulation have only been accomplished using adult samples (e.g., Ross and Ravosa, 1993; and see Lieberman et al., 2000), leaving unaddressed the ontogenetic causes underlying angular differences in adults. A popular hypothesis continues to be the spatial packing hypothesis (Ross and Ravosa, 1993), which describes "packing" of soft tissue regions within the cranium. Gould (1977) suggested that the great volume of the human brain, relative to the size (especially length) of the basicranium, produces a relatively flexed cranial base angle. Tests of the spatial packing hypothesis using mouse models affirm a relationship between brain size an basicranial flexion, and further suggest much of the variation in basicranial angle is explained by interactions between the size and dimensions of the basicranium and face (Hallgrímsson and Lieberman, 2008; Lieberman et al., 2008). Thus, much research supports this hypothesis, while also indicating other contributing factors affecting the cranial base (e.g., Weidenreich, 1941; Ross and Henneberg, 1995; Spoor, 1997; Strait and Ross, 1999; Lieberman et al., 2000).

While there have been large scale attempts to decipher different patterns in brain size among primates (e.g., Ross and Ravosa, 1993), fewer studies have examined synchondroses. Those that have examined synchondroses are biased toward anthropoids, and hominoids in particular (e.g., Schultz, 1940, 1941; Sirianni and Van Ness, 1978; Giles et al., 1981; Balolia, 2014; Joganic, 2016). Moreover, very few studies have examined synchondroses using histological methods (e.g., Baume, 1968; Michejda, 1972; Smith et al., 2017). This dearth of knowledge hinders our ability to determine how synchondroses influence the overall form of the primate cranium. What is known is that the sphenooccipital synchondrosis has prolonged patency in all primates studied to date (e.g., Schultz, 1940, 1941; Michejda, 1972; Sirianni and Van Ness, 1978; Giles et al., 1981; Joganic, 2016). This supports the argument that the sphenooccipital synchondrosis facilitates elongation of the posterior cranial fossa, and may influence cranial base angulation (Lieberman et al., 2000). However, there are several other midline synchondroses (**Table 1; Figure 1**) that have been postulated to influence basicranial angulation and/or midfacial orientation (Scott, 1953; Lieberman, 1998; Wealthall and Herring, 2006; Smith et al., 2017). Further, the possible role of bilateral synchondroses to influence the cranium globally, or the midface indirectly, has never been thoroughly explored.

The present study examines the joints of the developing basicranium in a wide spectrum of non-hominoid primates to address this gap in knowledge. Specifically, we use a combination of micro-CT reconstructions, serial histological sectioning, histochemical and immunohistochemical methods to describe the tissue composition of basicranial joints in several non-human primates of perinatal age. We seek to establish which cranial synchondroses, or hyaline cartilage between basicranial bones or between basicranial bones and septal cartilage, possess attributes of "growth centers" at birth. We identify growth centers as zones of chondrocyte hypertrophy and proliferation that typify epiphyseal plates (Hunziker, 1987) and have been documented in at least some cranial synchondroses (Wealthall and Herring, 2006; Cendekiawan et al., 2010). We use a perinatal sample to examine tissue mechanisms in patent (i.e., unfused) synchondroses. In addition to establishing joint types, we describe which cartilaginous joints possess characteristics of growth centers, such as zonal organization of chondrocytes and zone-specific production of matrix fibers.

Midline synchondroses with growth characteristics have been described between midline ossification centers in in many non-primates (e.g., Baume, 1968; Durham et al., 2017), and some nonhuman primates (Smith et al., 2017). In addition, mutations in fibroblast growth factor receptors are known, in several craniofacial syndromes, to greatly alter the form of the posterior cranial fossa through effects on endochondral bone growth (e.g., Driessen et al., 2017; Coll et al., 2019; and see Ornitz, 2005). Accordingly, we predict multiple growth centers are ubiquitous among midline basicranial articulations and among bilateral basicranial articulations of the posterior cranial fossa.

MATERIALS AND METHODS

A sample of 34 non-human primates were studied (Table 2), specifically seven species of strepsirrhines (including four lemur species, three bushbaby species) and six species of haplorhines (including Old and New World monkeys). Most specimens were of newborn age,

based on veterinary records or physical characteristics and cranial size when compared to specimens of known age for a particular species (see Smith et al., 2015). One baboon (*Paipo Anubis* was recorded at a preterm age of 168 days gestation, and was somewhat smaller than the other two specimens. Most specimens were scanned using micro-computed tomography (μCT), and subsequently histologically sectioned in sagittal, coronal or horizontal planes. A few specimens were examined by μCT alone, and some sectioned specimens were available from a previous study (Smith et al., 2017).

μCT scanning was conducted at Northeast Ohio Medical University (NEOMED) using a Scanco vivaCT 75 scanner (scan parameters: 70 kVp; 114 mA). The volumes were reconstructed using 20.5-30 μm cubic voxels and exported as 8-bit TIFF stacks for three-dimensional reconstructions (DeLeon and Smith, 2014; Smith et al., 2014). All three-dimensional reconstructions were carried out using Amira ® 2019.1 software.

Histological sectioning was conducted at Slippery Rock University (SRU) using routine paraffin embedding after decalcification in a formic acid-sodium citrate solution. Sections are 10 μm thick, and every fourth to tenth section was mounted on glass slides. Slides were alternately stained using Gomori trichrome or hematoxylin-eosin procedures (for more details see DeLeon and Smith, 2014).

Next, a second set of selected sections were mounted and stained for type II collagen using immunohistochemistry to qualitatively assess the relative amount of the most abundant collagen type in hyaline cartilage. Tissue for immunohistochemical staining was deparaffinized using xylenes and a graded ethanol series. These slides were rehydrated in phosphate buffered saline (PBS) followed by antigen retrieval performed by microwaving slides for three consecutive 5-minute periods at 20% power in a 1mM citrate solution, pH 6.0. Blocking of endogenous peroxidases was done by immersion in 1% H_2O_2 for 10 minutes. The slides were subsequently blocked by Millipore's proprietary blocking reagent for 1 hour at room temperature. Primary antibody omission was used as negative staining control. Tissue was stained using a mouse anti Col2A1 antibody (Collagen 2, Santa Cruz), 0.5μg/mL (1:200 dilution) overnight at 4°C. Detection of Col2A1 was performed using a Millipore proprietary secondary anti mouse and rabbit antibody (GT X Rb and Ms Igg) for 30 minutes at room temperature, Streptavidin HRP for 30 minutes, then 3, 3'- diaminobenzidine (DAB) substrate. Tissue was counterstained with VECTOR hematoxylin QS.

Most serial sections were examined by light microscopy using a Zeiss stereo microscope (X0.64 to X1.6 magnification) or a Leica DMLB photomicroscope (X25 to X630) to describe microanatomy of the synchondroses under study (see Table 1). Selected sections were photographed using an Axiocam MRc 5 Firewire camera (attached to the Leica microscope) or a MRc 150 Firewire camera (attached to the Zeiss microscope).

Finally, additional unstained sections were prepared at The Ohio State University College of Medicine (OSUMC) with Picrosirius red staining using a standard protocol (Durham et al., 2017). This method is useful for discerning collagen fiber orientation (Junqueira et al., 1978) and also fiber diameter (red = thick/mature; yellow = intermediate; green = thin/immature; Lattouf et al., 2014; Durham et al., 2017). Stained sections were photographed under polarized light using an inverted Olympus IX73 compound microscope with attached DP74 color CNOS Camera integrated into the capture workstation via Olympus CellSens software.

All articulations among chondrocranial elements (i.e., basicranial bones, plus nasal capsular bones or cartilage) were described microscopically according to tissue type and internal organization (**Table 3**). In total, eleven sites of articulation were examined (**Figure 1, Table 1**). Nomenclature for joints is based on the literature, with synonyms indicated (Baume, 1968; Balboni et al., 2005; Wealthall and Herring, 2006; Calendrelli et al., 2014; **Table 1**).

RESULTS

Strepsirrhini

Midline synchondroses (see Table 1 for key to abbreviations)

All strepsirrhines studied have three midline synchondroses with characteristics of active growth centers: the sphenooccipital synchondrosis (SOS), intrasphenoidal synchondrosis (ISS), and presphenoseptal synchondrosis (PSept). The SOS is a bipolar, longitudinal growth center between the basioccipital and basisphenoid (**Figs. 2a-c; 3a-c**). Zones of hypertrophic and proliferating chondrocytes are found at both anterior and posterior poles of the joint (**Figs. 2d, 3d**). Hypertrophic chondrocytes are organized into columns of 6 to 10 cells; proliferating chondrocytes are found in columns of eight to twelve cells. The resting zone is relatively broad. Picrosirius red preparations, viewed with polarized light microscopy, reveal the resting and proliferating zones have a predominantly dorsoventral orientation of collagen fibers (**Fig. 2e**), while fibers orient longitudinally in the hypertrophic zone. Reactivity to type II collagen antibodies is strongest in the resting and proliferating zones, with at least a slight decrease in the zone of hypertrophic chondrocytes (**Fig. 2f**).

In *Galago* and *Eulemur* spp., the SOS is continuous with a cartilaginous dorsum sellae (**Fig. 2c**). In contrast, in both *Varecia* spp. the dorsum sellae is ossified, and the SOS is symmetrical, and anteroposteriorly narrower (in relative dimensions) compared to *Galago* and *Eulemur* spp.

The ISS too, is a bipolar, longitudinal growth center, found between the basisphenoid and presphenoid centers of ossification (**Figs. 4a, b; 5a-c**). Zones of hypertrophic and proliferating chondrocytes are found at both anterior and posterior poles of the joint (**Figs. 4b, 5d**).

Hypertrophic and proliferating chondrocytes are organized into columns, similar in numbers to the SOS, though in some cases fewer or less organized (**Fig. 5d**). Picrosirius red preparations, viewed with polarized light microscopy, reveal the resting and proliferating zones have a predominantly dorsoventral orientation of mostly yellow and some red fibers (**Fig. 4c**), while yellow fibers orient longitudinally in the hypertrophic zone. In some regions, longitudinal fibers penetrate somewhat into the proliferating zone (**Fig. 4c**). Reactivity to type II collagen antibodies is strongest in the resting and proliferating zones, with more attenuated reactivity in the zone of hypertrophic chondrocytes (**Fig. 4d**). The specimen shown in **Figure 4c** and **d** has a central region that is denser with chondrocytes and consequently matrix-poor.

In comparison to the anteroposterior breadth of SOS, ISS varies. In *Galago* ISS is approximately equal to or less than the breadth of SOS (**Fig. 5a**). In *Eulemur* spp., the two synchondroses are similar in anteroposterior dimensions (not shown). In *Varecia* spp., the ISS is equal to or broader in anteroposterior dimensions than SOS (**Fig. 5b**).

The presphenoseptal synchondrosis (PSept) is a longitudinal, unipolar growth center (**Figs. 6a, b; 7a-c**). In some cases, the PSept may have a radial appearance (**Fig. 7c**). It is roughly parallel with the orientation of the more posterior synchondroses in lemurids, but inclines slightly ventrally in *Galago* spp. Hypertrophic and proliferating chondrocyte zones are seen in all species. Columns of hypertrophic chondrocytes contain more numerous cells than in proliferating zones, which have smaller clusters of cells. Picrosirius red preparations reveal a grid-like array of perpendicular red or yellow fibers that support most of the septal cartilage, but in the proliferating zone, some dorsoventrally aligned groups of fibers predominate (**Fig. 6c**). In the hypertrophic zone, collagen fibers orient longitudinally. Reactivity to type II collagen antibodies is strongest in the resting and proliferating zone, with more attenuated reactivity in the zone of hypertrophic chondrocytes (**Fig. 6d**).

Joints in the anterior cranial fossa differ in organization from SOS and ISS. There are two relevant locations where elements of the ethmoid bone unite with other cranial elements. The rostral edge of the orbitosphenoid (the central portion forming the jugum sphenoidale) is continuous with the posterosuperior septal cartilage, and more rostrally in the midline, the ethmoid may or may not have commenced ossification. In *Eulemur* spp., the perpendicular plate of the ethmoid remains unossified in the newborn. This is also true of *Varecia* (**Fig. 7b**). As such, there is cartilaginous continuity in the anterior cranial base between the dorsum of the sphenoid and septum (i.e., at the sphenoethmoidal synchondrosis). In *Galago* and *Otolemur*, ossification of the perpendicular plate has commenced. Thus in galagids, there is an expanse of septal cartilage connecting the perpendicular plate with the dorsum of the sphenoid. This site can be considered the midsagittal part of the sphenoethmoidal synchondrosis, but it differs from the more posterior synchondroses in that there are no proliferative chondrocyte zones typical of growth centers. The perpendicular plate itself takes the form of a crescent with the convex side

directed inferiorly (**Fig. 8a).** The perpendicular plate connects to ossifying parts of the cribriform plate that reside more laterally in the floor of the anterior cranial (olfactory) fossae (**Fig. 8b).** The perpendicular plate has a radial arc of chondrocyte hypertrophy on its septal interface (**Figs. 8c, d**). Proliferating chondrocytes are present, but in scattered clusters (**Fig. 8d**).

Bilateral synchondroses (see Table 1 for key to abbreviations)

In the anterior cranial fossa there are no bilateral synchondroses. There are three bilateral articulations between endochondral bones within the middle cranial fossa. The midline basisphenoid articulates with the bilateral alisphenoid bones. In some newborn strepsirrhines, this interface has a synchondroseal component anteriorly, the alibasisphenoidal synchondrosis (ABS; **Figs. 9a, b**), and posteriorly a shorter fibrous articulation is found. In Figure 1, these two parts are seen at joint # 6 (the wider more anterior gap is the synchondrosis). Posterior to the ABS articulations in the middle cranial fossa, the basisphenoid is adjacent to the petrous temporal, but only fibrous connective tissue intervenes between them (not shown; **Table 3**).

Within the posterior cranial fossa there are multiple sites of articulation among endochondral bones. The bilateral petrooccipital articulation, between the basioccipital and petrous temporal bones, is solely a fibrous joint (Suppl. Fig. 1). In contrast, there are three bipolar synchondroses associated with the exoccipital. Anteriorly, the anterior intraoccipital synchondrosis (AIOS) is between the basioccipital and the exoccipital (**Fig. 9c**). The JS is between the exoccipital and the temporal bone (**Fig. 9d**). The posterior intraoccipital synchondrosis (PIOS) is between the exoccipital and the temporal bone (**Fig. 9e**).

The ABS is variable among newborn strepsirrhines (**Fig. 10**). In *Eulemur* spp. no cartilage was seen at the ABS site in most specimens. However, in one smaller *E. collaris* specimen a small, quadrate (in coronal sectional view) cartilage intervenes between the basitrabecular process of the basisphenoid and the medial part of the alisphenoid (**Figs. 10a, b**). The presence of the Vidian nerve ventral to this site (**Fig. 10b**) establishes that this location corresponds to the ABS of galagids (**Fig. 10e**)

In galagids, the ABS sits in a horizontal (transverse) plane, which presents as a broad, quadrilateral cartilaginous plate in all newborn galagids (**Fig. 9b**). In the coronal plane it is narrower (**Figs. 10c-e**), thus the ABS takes the form of a flattened plate. The chondrocyte zones are bipolar and well organized into columns of proliferation and hypertrophy that generally orient transversely (**Figs. 9b, 10c-e**) but slightly anteriorly (**Fig. 10b**). In coronal cross-section, collagen fiber orientation resembles that observed in bipolar midline synchondroses (**Fig. 10d**) and the distribution of type II collagen is similar (**Fig. 10e**).

All of the synchondroses of the posterior cranial fossa exhibit characteristics of active growth centers. In the AIOS and PIOS, hypertrophic and proliferating chondrocytes are well

organized into columnar streams (**Fig. 10c, e**). Both of these synchondroses have an anteroposterior orientation when viewed in either horizontal (**Fig. 10**) or sagittal (**Fig. 11**) planes. However, the horizontal sections also show that the AIOS orients anteromedially (**Fig. 10c**) and the PIOS orients anterolaterally with some curvature of the overall shape in the horizontal plane (**Fig. 10e**). In addition, AIOS is continuous posteriorly with the cartilage of the ventrally expanding occipital condyle (**Fig. 11a**). The JS has chondrocyte hypertrophy at both interfaces. Proliferating cells were notably indistinct, but this may relate to the plane of section (**Fig. 10d**). The axis of growth is superoinferior. However, most of the JS also orients laterally.

Haplorhini

Midline synchondroses

Similar to strepsirrhines, in New World (NW) and Old World (OW) monkeys, at least same three midline synchondroses had characteristics of a growth center. In between the basisphenoid and basioccipital is the SOS, a bipolar longitudinal growth center, with hypertrophic and proliferating chondrocytes on anterior and posterior sides stacked in columns (**Figs. 12a-d; 13a-c**). Picrosirius red staining viewed with polarized light microscopy reveals that resting and proliferating zones have predominantly dorsoventral orientation of collagen fibers (**Figs. 12e; 13d**), with fibers oriented longitudinally in hypertrophic zones. Fibers appear yellow to red in *Macaca*, and orange to red in *Saguinus.* Reactivity of type II collagen antibodies is strongest in the resting and proliferating zone, with a sharp decrease in the zone of hypertrophic chondrocytes (**Figs. 12f, 13f**).

ISS is a bipolar growth center between basisphenoid and presphenoid (**Figs. 14a-e; 15a-d**). Hypertrophic and proliferating chondrocytes are on anterior and posterior sides of ISS, arranged in columns (**Figs. 14e; 15a**). Picrosirius red staining viewed with polarized light microscopy reveals resting and proliferating zones having dorsoventral orientation of collagen fibers (**Figs. 14d; 15b**), with fibers oriented longitudinally in hypertrophic zones. Some regions have longitudinal fibers penetrating into proliferating zones. Fibers appear orange to red. Reactivity to type II collagen antibodies is strongest in resting and proliferating zones, with decreased reactivity in the zone of hypertrophic chondrocytes (**Figs. 14c; 15d**).

Between the presphenoid and cartilaginous septum, the PSept is a longitudinal, unipolar growth center (**Figs. 16a-d; 17a-d**). In *Macaca mulatta, Saguinus oedipus,* and *Saimiri boliviensis*, this synchondrosis is oriented anteroinferiorly with a radial appearance as opposed to longitudinal. The radial orientation is most pronounced in some, but not all *Saimiri* specimens (**Fig 17c, d**), but in all cases it is oriented anteroventrally. Hypertrophic and proliferating chondrocytes are present in all species. Proliferating chondrocytes have much smaller columns (i.e., with fewer cells) than hypertrophic chondrocytes (**Figs. 16b; 17a**). Picrosirius red staining viewed with polarized light microscopy reveals variable collagen fiber orientation for the *M.*

mulatta, but in the synchondrosis, near to proliferating chondrocytes, some fibers groups run parallel to the synchondrosis. In the hypertrophic zone, fibers are oriented dorsoventrally (**Fig 16c**). Fibers running parallel to PSept were not as apparent in *Papio* (not shown). In all species, the septal cartilage has red and yellow collagen fibers arranged in a grid-like fashion (**Fig 17b**). Reactivity to type II collagen antibodies was strongest in the resting and proliferating zones with decreased presence of type II collagen in the hypertrophic zone (**Figs. 15d; 16d**).

In the anterior cranial base, septal cartilage appears to closely approach the orbitosphenoid in *Papio*. In the smaller, premature stillborn specimen, there is direct continuity of the orbitosphenoid (at the jugum) and posterior septal cartilage (not shown). In the newborn *Papio*, a small portion of the septum meets the periosteum of the orbitosphenoid (**Fig. 18a**). No columns of proliferating and hypertrophic chondrocytes were observed in this region of septal cartilage. In newborn *Macaca,* no septal cartilage meets the jugum, and instead only fibrous connective tissue is observed (as schematically shown in Fig. 1b). The perpendicular plate of the ethmoid has commenced ossification in *Papio*, and ESept is a radial endochondral growth center orienting ventrally from the bone's edge (**Figs. 18a, b**). The perpendicular plate is anchored to the jugum by a collagenous membrane (**Fig. 18c**). ESept has hypertrophic chondrocytes and spare proliferating chondrocytes (**Fig. 18b**). In contrast, no hypertrophic chondrocytes are visible in the cartilage adjacent to the presphenoid (**Fig. 18d**).

In *Saguinus* and *Saimiri*, there is no cartilaginous continuity of septal cartilage with the presphenoid at the site of sphenoethmoidal synchondrosis (**Figs. 19a-h**). Contact between the septum and the presphenoid is maintained only ventral to the anterior cranial base, at PSept (**Figs. 19c, d, g, h**). At the level of the anterior cranial base, there is only a narrow gap in which the cartilaginous septum can articulate with the midline sphenoid at the jugum sphenoidale. Here, only fibrous tissue intervenes between the septum and presphenoid (**Figs. 19e, g, h**). This site is the union of the sphenoid and future ethmoid bone, often called the "sphenoethmoidal synchondrosis", but here in these monkeys lacks any features of a synchondrosis.

Bilateral synchondroses

In the anterior cranial fossa there are no bilateral synchondroses in any of the monkeys examined here. There are three bilateral articulations between endochondral bones within the middle cranial fossa (**Table 3**). The midline basisphenoid articulates with the bilateral alisphenoid bones with variation at the interface of the bones. In some newborn *Saguinus* and *Callithrix*, this joint is cartilaginous (**Figs. 20, 21**). Two of the eight *Saimiri* possess some cartilage at ABS (at least one specimen is likely late fetal, based on the small size). As in strepsirrhines, the cartilage connects the basitrabecular process of the basisphenoid with the alisphenoid, but in all anthropoids the orientation of the joint is more anterior, especially in the platyrrhines (**Figs. 20c; 21e**). The Vidian nerve has a close relationship to both the cartilage of

the ABS and the basitrabecular process of the basisphenoid. It enters the canal posteriorly, approaching the ABS from the ventral side (**Figs. 21c, d**). It exits the pterygoid canal with a slightly upward trajectory (**Fig. 21a, b**) en route to the pterygopalatine ganglion (**Fig. 21e**). As such, the Vidian nerve is useful for identifying the location of the ABS after fusion has occurred (**Fig. 21h**). In specimens where no cartilage is observed at the ABS site, the joint is fused, bridged by bone.

Horizontal sections reveal the ABS, in specimens in which it is cartilaginous, as having bipolar hypertrophic and proliferating zones (**Fig. 20d**). While in *Callithrix* the ABS is oriented in a horizontal plane (**Figs. 20c, d**), in *Saguinus* the ABS is oriented slightly inferiorly in addition to anteriorly (**Figs. 21 e, f**). In *Saimiri*, the orientation is the same, even after fusion (**Figs. 21g, h**). In both catarrhines, ABS remains cartilaginous, and sagittal sections reveal it is oriented anteriorly and inferiorly (Suppl. Fig. 2).

Posterior to the alibasiphenoidal articulations, both basioccipital and basisphenoid are adjacent to the petrous temporal (petrooccipital and sphenopetrosal joints, respectively), but only fibrous connective tissue intervenes between them (not shown; **Table 3**).

All of the synchondroses of the posterior cranial fossa have bipolar hypertrophic and proliferating zones. In the AIOS and PIOS these zones of chondrocytes are well organized into columnar streams (e.g., **Fig. 20e**). Both of these synchondroses have an anteroposterior orientation when viewed in either horizontal (**Fig. 20e**) or sagittal (**Fig. 22d**) planes. However, the horizontal sections also show that the AIOS orients medially from posterior to anterior (**Fig. 20a, e**), and at the resting zone the synchondrosis undergoes a pronounced curvature when viewed in the sagittal plane (**Fig. 22d**). Picrosirius red preparations of sagittal sections reveal complex fiber directions (**Fig. 22e**). AIOS is continuous posteriorly with the cartilage of the ventrally expanding occipital condyle (**Fig. 22a**). The PIOS exhibits the appearance of a typical bipolar growth center when viewed near the midline in the sagittal plane (**Fig. 22a, b**), with dorsoventrally oriented collagen fibers (**Fig. 22c**). The JS has chondrocyte hypertrophy at both interfaces and proliferating cells were visible on one side of the bipolar growth center when viewed in a coronal plane (**Fig. 22f, g**). The axis of growth is superoinferior and laterally.

DISCUSSION

The precise role of synchondroses in influencing basicranial form is far from clear. There are two possible modes of influence, either or both of which may be at work in producing cranial diversity. The first is the concept that some synchondroses can directly affect angularity through differential growth rates at the endocranial versus ectocranial sides of the joint (Scott, 1953; Michejda, 1972; Moore, 1981). Another concept is that the different timing of closure of these joints (via ossification that unites the participating bones) may influence angulation (Lieberman et al., 2000; Moore, 1981; Smith et al., 2017). Similarly, midfacial orientation could be affected by the differing shapes of synchondroses that cause directional variation in growth (Smith et al.,

2017); or, alternatively, midfacial orientation might be affected by the differing pace of growth of synchondroses (Lieberman 1998).

Much of what we know about cranial base angulation in primates is based on osteological or CT data from ontogenetic samples (e.g., Lieberman and McCarthy, 1999; McCarthy, 2001; Rijkin et al., 2015), most recently reviewed by Lieberman et al. (2000). However, the supporting data are incomplete in critical ways. Osteological data preferentially focus on patent growth centers, that is the SOS (e.g., Giles et al., 1981; Joganic, 2016), to the exclusion of other midline synchondroses. A further reason for this incomplete understanding is that the more anterior synchondroses are difficult to observe ectocranially. Another limitation is sampling bias toward anthropoids, and especially apes and humans. Thus, there is no basis for making assertions on functional roles of synchondroses in primates generally, because ontogeny of synchondroses has been studied in so few primate taxa. Finally, the cranial base has been studied histologically in even fewer primates, namely several Old World monkeys and humans (Baume, 1968; Michedja, 1972; Adams and Harkess, 1972; Heinkele et al.,1989). Thus, hypotheses regarding uniquely human attributes of the cranial base rely on an incomplete comparative perspective. In this report, we provided a critical first step of establishing where cartilaginous joints are found at birth in non-hominoid primates, and in which cases these joints possess characteristics of active growth centers. Below we discuss implications and limitations of our findings.

Overview of basicranial joints

Terminology of basicranial joints has been inconsistent. Balboni et al. (2005) discussed variable terms for the petrooccipital (petrous temporal-basioccipital) joint, including synchondrosis (Kreiborg and Bjork, 1982), fissure (e.g., Lee et al., 2001), suture (Kreiborg and Bjork, 1982), or complex (Singh et al., 1997). Another useful example is the human sphenoethmoidal joint which has been termed a synchondrosis (e.g., Lieberman et al., 2000), suture (Baume, 1968; Roche and Lewis, 1976), or point (i.e., "sphenoethmoid point," Sameshima and Smahel, 2000) depending on the source. Partially, these inconsistencies relate to variable terminology among anatomical disciplines of study (e.g., developmental, surgical, cephalometric). However, another factor is the paucity of postnatal human developmental material investigated by histological methods. Human cranial arthrology has primarily been conducted using gross osteological (e.g., Krogman, 1930; Cray et al., 2010) or radiological (e.g., Krieborg and Cohen, 1982; Rijkin et al., 2015; Calandrelli et al., 2014; Driessen et al., 2017) methods. Only rarely has basicranial material been studied histologically in humans (e.g., Melsen; Thilander and Ingervall, 1973) or non-human primates (e.g., Michedja, 1972; Heinkele et al., 1989). As a result, the tissue-level identity of basicranial joints is often inferential.

Modeling human growth by comparison to other mammals has advantages, one being that many other mammals possess the same synchondroses as humans (Cendekiawan et al., 2010), and thus rodents or other small mammals are tractable models for understanding the importance of growth centers. However, there are certain fundamental differences between the synchondroses of humans and other mammals. Baume (1968) described a basic difference in microstructure of the SES in rats and humans, where in the former, SES is described as a growth center, while in humans it is described as a suture. Experimental evidence demonstrates different roles in growth for fibrous joints (e.g., sutures) and synchondroseal growth centers (e.g., Rönning and Kylämarkula, 1982). Thus it seems critical to seek phylogenetic models that more

closely resemble humans. Still, even within the Order Primates it is suggested there are fundamental differences in the timing of synchondroseal fusion, either at SES (Lieberman et al. (2000) or ISS (Smith et al., 2017). Lieberman et al. (2000) suggested that differences in the timing of synchondroseal fusion may contribute to basicranial angularity, and specifically indicated SES fuses later in humans than all other primates. Data presented here offer insight into prenatal patterns of synchondroseal growth that manifest in the newborn, particularly regarding perinatal patency.

Within the cranial base, all primates studied possess at two midline synchondroses (SOS, ISS) and three bilateral synchondroses (AIOS, PIOS, JS) at birth, all of which remain cartilaginous and have cellular and matrix properties of active growth centers (Table 3). These synchondroses appear to have similar roles in basicranial growth among the primates studied here, in elongation of the midline and posterior cranial fossae (ISS, SOS), increasing the diameter of the foramen magnum (AIOS, PIOS), and increasing the global dimensions of the posterior cranial fossa (SOS, JS, AIOS, PIOS). Their roles in these dimensional growth patterns may be inferred to be significant prenatally and perinatally, but further study is required to establish the postnatal duration of their chondrocyte activities.

Together, the anthropoids and strepsirrhines studied here are distinct from humans at the ISS which has been documented to fuse perinatally in ourselves (Baume, 1968). But Smith et al. (2017) suggest this could be a trait shared by other hominoids, an assertion that requires histological study. Many studies have noted a potential link between anterior cranial base length and midfacial projection, but the discussion has been disproportionately focused on hominoids, or hominids specifically (e.g., Lieberman, 1998; Spoor et al., 1999; Lieberman et al., 2002). Our findings emphasize the need for a broader investigation of primates that reveals postnatal fate of sphenoidal synchondroses; further depth of knowledge may explain trends in basicranial growth and midfacial orientation in anthropoids.

Previously (Smith et al., 2017), we discussed the sphenoethmoidal articulation at the midface, and noted a radial growth center in anthropoids where the presphenoid articulates with the septum (i.e., PSept). Whereas this growth center, once ossified, will articulate with the ethmoid at the perpendicular plate, it is not equivalent with SES, as we implied. SES has explicitly been used to refer to a more dorsal articulation at the level of the anterior cranial fossa (see above). Here, we show this articulation follows a phylogenetic pattern that might distinguish anthropoids from all other primates. All anthropoids studied here lack direct cartilaginous continuity between the midline orbitosphenoid, which was ossified or nearly so at birth, and the cartilage of the ethmoid bone, including the posterosuperior ethmoid, part of the mesethmoid, which gives rise to the perpendicular plate of the ethmoid . All strepsirrhines exhibited continuity of the orbitosphenoid and ethmoidal cartilage, but SES lacks any characteristics of a growth center, at least at birth.

The pattern observed here also appears to pertain to humans (and perhaps all anthropoids). Baume (1968) provided clear, but often overlooked, evidence that SES undergoes fibrous degeneration perinatally. More specifically, the continuity of the median, rostral part of the sphenoid with mesethmoid cartilage is interrupted by cartilage at the sphenoethmoidal junction where the anterior cranial fossa transforms from cartilage to fibrous tissue. This type of tissue conversion is documented for other parts of the chondrocranium, such as the posterior

nasal capsule (Smith et al., in review). Our findings suggest this type of change may typify all anthropoids, although a larger series of developmental stages is needed to determine the precise mechanism of this conversion. Nonetheless, it appears SES may lack characteristics of a growth center in all primates at birth. Moreover, in anthropoids, it cannot be asserted to possess intrinsic growth potential at all, and instead functions like a suture, allowing passive growth as the brain expands within the anterior cranial fossa. Further ontogenetic work is needed to assess how long SES remains patent in anthropoids as there may be nothing distinct about prolonged patency at SES in humans as asserted by Liebermann et al. (2000).

Two additional midline synchondroses are found in most primates, PSept and ESept. Each has growth center characteristics, and each is spatially positioned to affect midfacial length and orientation. Using a larger breadth of species than Smith et al. (2017), we confirm the dichotomous nature of PSept in anthropoids (specifically monkeys) compared to strepsirrhines (bushbabies and lemurs), the significance of which will be discussed below. Here, the uniquely more inferior trajectory of PSept is confirmed on a larger sample of anthropoids; the radial shape is also confirmed, but the degrees of the arc vary interspecifically and intraspecifically. We also establish variability in the presence of an active ESept. There is no difference detected between anthropoids and strepsirrhines; both appear to vary in ESept activity at birth. At present, we assume this is explained as a different timing of ossification of the perpendicular plate in primates; in humans, ESept is active after birth, during early infancy (Baume, 1968).

Some of the bilateral joints not described above (petrooccipital, sphenopetrosal) are fibrous, and could properly be considered suture-like in function. Given the developmental sequence of SES in anthropoids, it remains an open question whether these may begin as cartilaginous joints and undergo fibrous conversion. One of the *Papio* specimens, born slightly prematurely, hints there is first a cartilaginous joint at SES, followed by orbitosphenoid ossification. Since the orbitosphenoid and septal cartilage are further separated in newborns, we hypothesize the joint becomes progressively more fibrous in monkeys during the perinatal period. The last remaining synchondrosis, ABS, is another variable joint among species. Of this joint, Maier explained "This synchondrosis is a functional joint and a center of growth at the same time (in German, "Wachstumsgelenk"). This important suture [it becomes so] does not even have an official anatomical name" (1993, p 172). Our findings are consistent with this view of an ontogenetic shift in joint type at the interface of the alisphenoid and basisphenoid. Only one family studied (Galagidae) possesses an active growth center in all specimens examined. Lemurids and callitrichines were more variable: some but not all specimens have cartilage at the site, and we tentatively interpret this to mean that conversion of the joint from synchondrosis to fibrous is a perinatal event. We thus regard the ABS to be of greatest significance as an active growth center during prenatal development.

Microstructure

Most synchondroses identified here had zonal organization that is typical of active growth centers (Hunziker et al., 1987; Kember, 1978). In nearly all of them, bipolar or unipolar zones of hypertrophic and proliferating chondrocytes were identified. The degree of organization into tight columns varied; longitudinal synchondroses had larger numbers of proliferating cells in columns than radial synchondroses. In some cases, proliferating cells may have been difficult to discern based on the plane of section (e.g., JS). Growth centers such as epiphyseal plates also

exhibit zone specific production of collagen fiber types (Durham et al., 2017). Here we demonstrate that in nearly all cases, type II collagen is widespread throughout the resting and proliferating zone in all synchondroses studied. In nearly all cases, the reactivity to type II collagen antibodies is reduced in the hypertrophic zone. This is consistent with previous work on cranial synchondroses and growth plates, in which type II collagen is degraded and type X collagen is produced in the hypertrophic zone (Alini et al., 1992; Römer et al., 2010). We also confirm that all longitudinal synchondroses have zone-specific orientation of collagen fibers, with dorsoventral organization within the resting zone and at least part of the proliferating zone, with a transition to longitudinal fibers in the hypertrophic zone. This is the same organization reported in the epiphyseal growth plate of long bones (Junqueira et al., 1978) and the SOS of growing macaques (Heinkele et al., 1989). Radial synchondroses exhibit a more latticework organization of fibers in common with the remainder of the septum, with some locations having organized bundles that run nearly parallel to PSept.

The arrangement of type II and other forms of collagen within the hyaline cartilage matrix is becoming increasingly well-understood (Bruckner and van der Rest, 1994; Talts et al., 1998), but biomechanical properties are still the subject of much discussion. It is thought that initially, thin collagen fibrils are formed, and these primary fibrils become secondarily fused, increasing the fiber diameter (Bruckner and van der Rest, 1994). Fiber diameter is also augmented by linkage of other collagen types (type IX and XI are smaller collagen molecules known to fuse to type II collagen). We offer no particular interpretation of the proportion of fiber types in the specimens studied, except to note since all species had at least some "mature" (red) fibers in addition to intermediate fibers, a reorganization of the primary fibrils is underway in all species. This is unsurprising to the extent that matrix production begins prenatally, and because primates have relatively prolonged gestations (Portmann, 1941; Martin, 1990), although with much interspecific variation. Fiber diameter does not vary significantly across species (Bruckner and van der Rest, 1994). In terms of the arrangement of fibers, Bruckner and van der Rest (1994) liken the function of these fibers to role of concrete rods in concrete (with ground substance likened to the aggregate plus water in concrete). It is apparent that two distinct patterns are revealed in the cartilages examined: the dorsoventrally oriented, parallel bands of fibers in resting and proliferating zones, and the latticework organization seen throughout most of the septum. In the synchondroses, the former have been previously described in SOS of OW monkeys (Heinkele et al., 1989). This appears to represent a peak plateau point along an arc of fibers that anchors to bone at the ossification front. Type II collagen forms the majority of normal cartilage extracellular matrix, and its absence (e.g., in mutant mouse strains) results in absence of growth plates (Talts et al., 1998). Thus, the arrangement observed in resting and proliferative zones is likely an important hallmark of growth centers. The latticework arrangement within the septum is somewhat reminiscent of that described for type X collagen in hyaline cartilage (Bruckner and van der Rest, 1994), and may provide more generalized stability.

With the exceptions of ISS and ABS, most of the synchondroses that were patent in anthropoids also remain patent for at least one to four years in humans (Scheuer and Black, 2004). In that sense, it is not surprising that most of the synchondroses identified here possess characteristics consistent with active growth centers. However, patency is not a sufficient indicator of synchondroseal growth (Thilander and Ingervall, 1973), and non-histological methods may fail even to detect patency (Adams and Harkess, 1972). Thus, the histological

observations provided give us confirmation of active growth at birth across most of the cartilaginous joints of the cranial base (Table 3). As synchondroseal growth slows (e.g., with aging), there are important tissue level changes that occur. In Old World monkeys, the chondrocyte density in the resting zone reduces and the cartilage matrix becomes increasingly mineralized in the SOS as it ceases growth activities (Heinkele et al., 1989). In some mammals, synchondroses do not fuse, but there are still cartilage matrix changes and decreased cellularity (Roach et al., 2003). Fusion first occurs across the ventral side of SOS in macaques (Adams and Harkess, 1972). We detected no similar changes consistent with growth cessation with any synchondroses aside from ABS and SES (see below). Thus, further study must assess the fate of these synchondroses across postnatal age. In addition, the growth rates at these joints must be measured according to histomorphometric aspects of chondrocyte zones (e.g., see Kembell, 1978), especially given some apparent variation in the number of proliferating cells among synchondroses.

Driving or drifting

Cartilage-dependent mechanisms for basicranial and facial growth have been extensively discussed (e.g., Scott, 1953, 1954; Hoyte, 1973; Wealthall and Herring, 2006). In young growing mice, the rate of mineralization in the SOS is essentially equal to the rate at which new cartilage matrix is produced (Wealthall and Herring, 2006). In this manner, interstitial cartilage growth during endochondral ossification increases basicranial length and, to a lesser extent, basicranial width. In adult mice, at least some synchondroses remain cartilaginous into adult ages, but they cease to promote growth (Roach et al., 2003). In both humans and macaques, synchondroseal growth is most accelerated at younger ages (Thilander and Ingervall, 1973; Giles et al., 1981; Heinkele et al., 1989). However, cartilage remains at the site for some time before there is osseous fusion across the joint. For this reason, patency of synchondroses does not signify active cartilaginous growth (Thilander and Ingervall, 1973; Heinkele et al., 1989).

Concerning basicranial form, it has been postulated that synchondroses can directly affect angularity through differential growth rates at the endocranial versus ectocranial sides of the joint (Scott, 1953; Michejda, 1972; Moore, 1981). More data, including examination of additional stages of development, are required before this might be confirmed. While we can draw little inference about differential growth at SOS and ISS, monkeys have a notably more angular or radial PSept than lemurs at birth. Possible implications are that growth is more rapid along the more superior part of PSept prenatally, or that this downward angularity is established in the primordial chondrocranium. A final consideration is that the nasal septal cartilage itself has long been implicated as a driver of midfacial growth, with some disagreement on the timing or extent that it contributes (e.g., Scott, 1953; Melsen, 1977; Siegel et al., 1990; Van Loosen et al., 1996; Foster et al., 2016; Smith et al., 2017). This potentially creates an added dynamic in facial growth. Indeed, Wealthall and Herring's (2006) study of mice revealed two means by which the septal cartilage may generate tissue-separating forces: endochondral ossification of the septum and interstitial growth. They calculate that septal growth exceeds the amount that would be calculated by endochondral ossification alone. They conclude that while chondrocyte hypertrophy and proliferation at PSept and ESept increase septal dimensions, additional growth occurs throughout the remainder of the septum via interstitial expansion. This is supported by

widespread chondrocyte proliferation in the septal cartilage (i.e., as opposed to the restricted zone specific proliferation in the synchondroseal growth centers).

All synchondroseal growth centers are limited in their intrinsic growth potential. Therefore, the prolonged changes in basicranial angulation observed in catarrhines (Lieberman and McCarthy, 1999; Sirianni and Van Ness, 1978) may be partially explained by bone drift that occurs after synchondroseal fusion via bone modeling. In this sense, timing of cessation of growth at synchondroses is of critical importance since intrinsic growth potential no longer exists. Our study demonstrates the need to establish the timing that synchondroseal growth ceases across a broad array of primates. Already, we can point to two synchondroses that vary in a significant manner at birth. First, SES may have an unusual trajectory in all anthropoids in its conversion to a fibrous joint. We posit that loss of the synchondrosis between the sphenoid and ethmoid in the anterior cranial base may relate to the relatively large size and correspondingly fast growth of the frontal lobes in anthropoids. Further work is needed as our data presents no evidence of an active growth center at SES in newborn strepsirrhines.

Among bilateral synchondroses, ABS has two distinctions among primates. First, because only one smaller (possibly late fetal) lemur possessed any vestige of cartilage at ABS, we conclude the synchondrosis may lose active growth potential in lemurids just before birth. This means that postnatally, the middle cranial fossa changes dimensions and shape only via bone modeling in lemurs. All bushbabies, in contrast, maintain the capacity for endochondral growth at ABS at birth. This distinction may allow inferences about the relationship of ABS growth cessation relative to other variables, such as brain growth rate.

ABS was cartilaginous at birth in some, but not all newborn anthropoids. We therefore conclude that loss of cartilage (via ossification) is perinatal. One basic dichotomy among the primates studied. In strepsirrhines with cartilage at ABS, the growth trajectory was mainly lateral and slightly anterior. In anthropoids, growth was mainly anterior and slightly lateral. This suggests there is a fundamental change in alisphenoid orientation that relates at least in part to different synchondroseal growth trajectories. Further work is needed to understand development of lateral basicranial joints, especially in light of these early differences and the previous finding of a strong correlation between facial form and lateral regions of the basicranium (Bastir and Rosas, 2006).

Conclusions

Three midline synchondroses, SOS, ISS, and PSept act as growth centers at birth in all non-hominoid primates investigated here. In no instance are these synchondroses showing early signs of fibrous or osseous bridging at birth. In contrast, the SES exhibits no characteristic of an active growth center, nor is it fused, in any newborn primate studied. Instead, the sphenoid articulates with posterior septal cartilage in strepsirrhines, while in monkeys the SES exists as a "suture like" joint in the anterior cranial fossa, similar to Baume's (1968) nomenclature of this joint in newborn humans, as the "sphenoethmoidal suture." We can reject the hypothesis that angular differences in the basicranium among primates relates to the different timing of fusion of SES (Lieberman et al., 2000). Indeed, the idea that SES has a distinctly prolonged patency in humans (Lieberman et al., 2000) must now be re-evaluated. Postnatal ontogeny of SOS and ISS must be studied to assess the likelihood that differential growth within the synchondroses affects basicranial angularity.

The sphenoethmoidal articulations are complicated by the different timing of mesethmoid ossification among primates, as clearly indicated by perinatal ossification of the perpendicular plate in some (e.g., *Galago, Papio*) but not all species. The importance of PSept and ESept, both active growth centers, in modifying facial orientation, must also be explored ontogenetically. The distinctive form of PSept in anthropoids at birth (Smith et al., 2017) is confirmed in additional species, supporting the hypothesis that the ventrally displaced angle and/or the shape of PSept are likely important influencers of midfacial orientation (Smith et al., 2017). Yet, hominoids may lack a growth center at PSept (Baume, 1968; Smith et al., 2017). Given that, fibrous degeneration of cartilage at SES may be critical to explaining midfacial reductions in all anthropoids.

Lastly, here we describe four active growth centers in the middle and posterior cranial fossa. Their presence requires a careful consideration that early interstitial expansion of synchondroses may contribute to early postnatal basicranial form and midfacial orientation, and the timing in which these fuse may also provide an additional means by which the bilateral basicranial joints may globally affect cranial morphology (Bastir and Rosas, 2006; Neaux et al., 2013).

Acknowledgements

This is DLC publication # XXX.

LITERATURE CITED

Adams, D., & Harkness, M. (1972). Histological and radiographic study of the spheno-occipital synchondrosis in cynomolgus monkeys, *Macaque irus*. *The Anatomical Record*, 172(2), 127-136.

Alini, M., Matsui, Y., Dodge, G. R., & Poole, A. R. (1992). The extracellular matrix of cartilage in the growth plate before and during calcification: changes in composition and degradation of type II collagen. *Calcified Tissue International*, 50(4), 327-335.

Balboni, A. L., Estenson, T. L., Reidenberg, J. S., Bergemann, A. D., & Laitman, J. T. (2005). Assessing age-related ossification of the petro-occipital fissure: laying the foundation for understanding the clinicopathologies of the cranial base. *The Anatomical Record*, 282(1), 38–48

Balolia, K. (2014). Brief communication: The timing of spheno-occipital fusion in hominoids. *American Journal of Physical Anthropology,* 156:132-138.

Bastir, M., & Rosas, A. (2006). Correlated variation between the lateral basicranium and the face: A geometric morphometric study in different human groups. *Archives of Oral Biology*. 51(9), 814-824.

Baume, L. J. (1968). Patterns of cephalofacial growth and development. A comparative study of the basicranial growth centers in rat and man. *International Dental Journal*, 18(3), 489-513.

Bruckner, P., and van der Rest, M. (1994). Structure and function of cartilage collagens. *Microscopy Research and Technique,* 28, 378-384.

Calandrelli, R., D'Apolito, G., Gaudion, S., Sciandra, M. C., Caldarelli, M., & Colosimo, C. (2014). Identification of skull base sutures and craniofacial anomalies in children with craniosynostosis: utility of multidetector CT. *La Radiologia Medica*, 119(9), 694-704.

Cendekiawan, T., Wong, R. W. K., & Rabie, A. B. M. (2010). Relationships between cranial base synchondroses and craniofacial development: a review. *The Open Anatomy Journal*, 2(1), 67-75.

Coll, G., Rabbo, F.A., Jecko, V., Sakka, L., Di Rocco, F., and Delion, M. (2019). The growth of the posterior cranial fossa in FGFR2-induced faciocraniosynostosis: A review. *Neurochirurgie*, 65, 221-227.

Cray, J. Jr., Mooney, M. P., & Siegel, M. I. (2010). Timing of ectocranial suture activity in Pan troglodytes as related to cranial volume and dental eruption. *The Anatomical Record: Advances in Integrative Anatomy and Evolutionary Biology,* 293(8), 1289-1296.

DeLeon, V. B., & Smith T.D.. (2014). Mapping the nasal airways: using histology to enhance CT-based three-dimensional reconstruction in *Nycticebus*. *Anatomical Record*, 297, 2113–2120.

Driessen, C., Rijken, B. F., Doerga, P. N., Dremmen, M. H., Joosten, K. F., & Mathijssen, I. (2017). The effect of early fusion of the spheno-occipital synchondrosis on midface hypoplasia and obstructive sleep apnea in patients with Crouzon syndrome. *Journal of Cranio-Maxillo-Facial Surgery*, 45(7), 1069-1073.

Durham, E., Howie, R. N., Parsons, T., Bennfors, G., Black, L., Weinberg, S. M., Elsalanty, M., Yu, J. C., & Cray, J. J. (2017). Thyroxine exposure effects on the cranial base. *Calcified Tissue International*, 101(3), 300–311.

Enlow, D. H. (1976). The prenatal and postnatal growth of the human basicranium. In *Symposium on Development of the Basicranium* (pp. 192-205). US Department of Health, Education, and Welfare, Public Health Service, National Institutes of Health.

Ford, E. H. R. (1958). Growth of the human cranial base. *The American Journal of Orthodontics and Dentofacial Orthopedics*, 44(7), 498-506.

Foster, A., & Holton, N. (2016). Variation in the developmental and morphological interaction between the nasal septum and facial skeleton. *The Anatomical Record,* 299(6), 730–740.

Giles, W. B., Phillips, C. L., & Joondeph, D. R. (1981). Growth in the basicranial synchondroses of adolescent Macaca mulatta. *The Anatomical Record*, 199(2), 259-266.

Gould, S. J. (1977). *Ontogeny and phylogeny*. Cambridge. Belknap.

Hall, B. K. (2015). *Bones and cartilage*. (2nd ed.). New York: Academic Press.

Hall, B. K., & Precious, D. S. (2013). Cleft lip, nose, and palate: the nasal septum as the pacemaker for midfacial growth. *Oral Surgery, Oral Medicine, Oral Pathology, Oral Radiology, and Endodontology*, 115(4), 442–447.

Hallgrímsson, B. and Lieberman, D.E. (2008). Mouse models and the evolutionary developmental biology of the skull. *Integrative and Comparative Biology* 48, 373-384.

Heinkele, M., Freiburg, R., & Ewers, K. (1989). Die Synchondrosis sphenooccipitalis — eine fluoreszenz-und polarisationsmikroskopische Untersuchung am Cercopithecus-aethiops-Affen. *Fortschritte der Kieferorthopädie*, 50, 493-505.

Hoyte, D. A. N. (1973). Basicranial elongation: 2. Is there differential growth within a synchondrosis? *The Anatomical Record*, 175, 347.

Hunziker, E. B., Schenk, R. K., & Cruz-Orive, L. M. (1987). Quantitation of chondrocyte performance in growth-plate cartilage during longitudinal bone growth. *The Journal of Bone and Joint Surgery*, 69(2), 1621-173.

Jeffery, N. (2005). Cranial base angulation and growth of the human fetal pharynx. *The Anatomical Record*, 284(1), 491-499.

Jeffery, N., & Spoor F. (2002). Brain size and the human cranial base: a prenatal perspective. *The American Journal of Physical Anthropology*, 118(4), 324-340.

Joganic, J. L. (2016). Brief communication: Skeletal and dental development in a sub-adult western lowland gorilla (*Gorilla gorilla gorilla*). *American Journal of Physical Anthropology*, 159(1), 174-181.

Junqueira, L. C. U., Cossermelli, W. A., & Brentani, R. (1978). Differential staining of collagens type I, II and III by Sirius Red and polarization microscopy. *Archivum histologicum japonicum*, 41(3), 267-274.

Kember, N. F. (1978). Cell kinetics and the control of long bone growth. *Cell Proliferation*, 11(5), 477-485.f

Kjaer, I. (1990). Ossification of the human fetal basicranium. *Journal of Craniofacial Genetics and Developmental Biology*, 10(1), 29-38.

Kreiborg, S., & Bjork, A. (1982). Description of a dry skull with Crouzon syndrome. *Scandinavian Journal of Plastic and Reconstructive Surgery*, 16(3), 245–253.

Krogman, W. M. (1930). Studies in growth changes in the skull and face of anthropoids. II. Ectocranial and endocranial suture closure in anthropoids and Old World apes. *American Journal of Anatomy*, 46(2), 315-353.

Lattouf, R. Younes, R. F., Lutomski, D., Naaman, N. B., Godaeu, G., Senni, K., & Changotade, S. (2014). A useful tool to appraise collagen networks in normal and pathological tissues. *Journal of Histochemistry and Cytochemistry*, 62, 751-758.

Lee, S.K., Park, K., Kong, D.S., Cho, Y.S., Baek, C.H., Nam, D.H., Lee, J.I., Hong, S.C., Shin, H.J., Eoh, W., & Kim, J.H. (2001). Surgical tactics and outcome of treatment in jugular foramen schwannomas. *Journal of Clinical Neuroscience*, 1, 32–39.

Lieberman, D. E. (1998). Sphenoid shortening and the evolution of modern human cranial shape. *Nature*, 393(6681), 158-162.

Lieberman, D. E., & McCarthy, R. C. (1999). The ontogeny of cranial base angulation in humans and chimpan-zees and its implications for reconstructing pharyngeal dimensions. *The Journal of Human Evolution*, 36(5), 487–517.

Lieberman, D. E., Ross, C. F., & Ravosa, M. J. (2000). The primate cranial base: ontogeny, function, and integration. *Yearbook of Physical Anthropology*, 43, 117-169.

Lieberman, D.E., McBratney, D.M., and Krovitz, G. (2002). The evolution and development of cranial form in *Homo sapiens. PNAS*, 99, 1134-1139.

Lieberman, D.E., Hallgrímsson, B., Liu, W., Parsons, T.E. and Jamniczky H.A. (2008). Spatial packing, cranial base angulation, and craniofacial shape variation in the mammalian skull: testing a new model using mice. *Journal of Anatomy*, 212, 720-735.

Maier, W. (1993). Cranial morphology of the therian common ancestor, as suggested by the adaptations of neonate marsupials. In *Mammal phylogeny* (pp. 165-181). Springer, New York, NY.

Martin, R.D. (1990). *Primate origins and evolution. A phylogenetic reconstruction*. Princeton, NJ: Princeton University Press.

McBratney-Owen, B., & Lieberman, D. E. (2003). Postnatal ontogeny of facial position in *Homo sapiens* and *Pan troglodytes*. In: Patterns of growth and development in the genus *Homo.* Thompson, Krovitz, Nelsen (eds.) Cambridge: Cambridge University Press. P 45-72.

McCarthy, R. C. (2001). Anthropoid cranial base architecture and scaling relationships. *The Journal of Human Evolution*, 40(1), 41–66.

Melsen, B. (1974). The cranial base: the postnatal development of the cranial base studied histologically on human autopsy material. *Acta Odontologica Scandinavica,* 32(62), 9-126.

Melsen, B. (1977). Histological analysis of the postnatal development of the nasal septum. *The Angle Orthodontist*, 47(2), 83-96.

Michejda, M. (1972). The role of basicranial synchondroses in flexure processes and ontogenetic development of the skull base. *The American Journal of Physical Anthropology*, 37(1), 143–150.

Moore, W. J. (1981). *The mammalian skull*. Cambridge University Press.

Neaux, D., Guy, F., & Gilissen, E. (2013). Covariation between midline cranial base, lateral basicranium, and face in modern humans and chimpanzees: a 3D geometric morphometric analysis. *The Anatomical Record*, 296(4), 568-579.

Ornitz, D.M. (2005). FGR signaling in the developing endochondral skeleton. *Cytokine Growth Factor Reviews,* 16: 205-213.

Portmann, A. (1941). Die Tragzeiten der Primaten und die Dauer der Schwangerschaft beim Menschen: Ein Problem der vergleichenden Biologie. *Revue Suisse de Zoologie*, 48:511–518.

Rijkin, B. F. M., Lequin, M. H., Van Veelen M. L. C., de Rooi, J., & Mathijssen, I. M. J. (2015). The formation of the foramen magnum and its role in developing ventriculomegaly and Chiari I malformation in children with craniosynostosis syndromes. *Journal of Cranio-Maxillo-Facial Surgery*, 43(7), 1042-1048.

Roach, H. I., Mehta, G., Oreffo, R. O. C., Clarke, N. M. P., & Cooper, C. (2003). Temporal analysis of rat growth with age despite presence of a physis. *Journal of Histochemistry & Cytochemistry*, 51(3), 373–383.

Roche, A. F., & Lewis, A. B. (1976). Late growth changes in the cranial base. In *Symposium on Development of the Basicranium. Bethesda, MD: US Dept. Health, Education, and Welfare, NIH,* (pp. 221-239).

Römer, P., Weingärtner, J., Roldán, J.C., Proff, P., & Reicheneder, C. (2010). Development dependent collagen gene expression in the rat cranial base growth plate. *Annals of Anatomy* 192(4), 205–209.

Rönning, O., & Kylämarkula, S. (1982). Morphogenetic potential of rat growth cartilages as isogeneic transplants in the interparietal suture area. *Archives of Oral Biology*, 27(7), 581-588.

Ross, C., & Henneberg, M. (1995). Basicranial flexion, relative brain size, and facial kyphosis in Homo sapiens and some fossil hominids. *The American Journal of Physical Anthropology*, 98(4), 575–593.

Ross, C. F., & Ravosa, M. J. (1993). Basicranial flexion, relative brain size and facial kyphosis in nonhuman primates. *The American Journal of Physical Anthropology*, 91(3), 305–324.

Sameshima, G. T., & Smahel, Z. (2000). Facial Growth in Adulthood after Primary Periosteoplasty or Primary Bone Grafting in UCLP. *The Cleft Palate-Craniofacial Journal*, 37(4), 379-384.

Schultz, A. H. (1940). Growth and development of the chimpanzee. *Carnegie Institution of Washington Publication 518, Contributions to Embryology*, 28, 1-63.

Schultz, A. H. (1941). *Growth and development of the Orang-Utan. Carnegie Institution of Washington Publication 525, Contributions to Embryology*, 29, 57-110.
Scott, J. H. (1953). The cartilage of the nasal septum. *British Dental Journal*, 95, 37–43.

Siegel, M. I., Mooney, M. P., Eichberg, J. W., Gest, T., & Lee, D. R. (1990). Septopremaxillary ligament resection and midfacial growth in a chimpanzee animal model. *The Journal of Craniofacial Surgery*, 1(4), 182–186.

Singh, G. D., McNamara, J. A., Jr., & Lozanoff, S. (1997). Finite element analysis of the cranial base in subjects with class III malocclusion. *British Journal of Orthodontics*, 24(2), 103–112.

Sirianni, J. E., & Van Ness, A. L. (1978). Postnatal growth of the cranial base in *Macaca nemistrina*. *The American Journal of Physical Anthropology*, 49(3), 329-340.

Smith, T. D., Kentzel, E. S., Cunningham, J. M., Bruening, A. E., Jankord, K. D., Trupp, S. J., Bonar, C. J., Rehorek, S. J., & DeLeon, V. B. (2014). Mapping bone cell distributions to assess ontogenetic origin of primate midfacial form. *American Journal of Physical Anthropology*, 154(3), 424-435.

Smith, T.D., Jankord, K.D., Progar, A.J., Bonar, C.J., Evans, S., Williams, L., Vinyard, C.J. and DeLeon, V.B. (2015). Dental maturation, eruption, and gingival emergence in the upper jaw of newborn primates. *The Anatomical Record* 298, 2098–2131.

Smith, T. D., McMahon, M. J., Millen, M. E., Llera, C., Engel, S. M., Li, L., Bhatanagar, K.P., Burrows, A. M., Zumpano, M. P., & DeLeon, V. B. (2017). Growth and development at the sphenoethmoidal junction in perinatal primates. *The Anatomical Record,* 300(12), 2115-2137.

Smith, T. D., Ufelle, A., Cray, J. J., Rehorek, S. B., & DeLeon, V.B. Sphenoethmoidal integration is accelerated in primates. *The Anatomical Record,* In review.

Spoor, F. (1997). Basicranial architecture and relative brain size of Sts 5 (Australopithecus africanus) and other Plio-Pleistocene hominids. *South African Journal of Science*, 93(4), 182-187.

Spoor, F., O'Higgins, P., Dean, C., and Lieberman, D.E. (1999). Anterior sphenoid in modern humans. *Nature,* 397, 572.

Strait, D. S., & Ross, C. F. (1999). Kinematic data on primate head and neck posture: Implications for the evolution of basicranial flexion and an evaluation of registration planes used in paleoanthropology. *The American Journal of Physical Anthropology*, 108(2), 205-222.

Talts, J.F., Pfeifer A., Hofmann, F., Hunziker, E.B., Zhou, X.H., Aszódi, A., and Fässler R. (1998). Endochondral ossification is dependent on the mechanical properties of cartilage tissue and on intracellular signals in chondrocytes. *Annals of the New York Academy of Sciences*, 23, 74-85.

Thilander, B., & Ingervall, B. (1973). The human spheno-occipital synchondrosis II. A histological and microradiolic study of its growth. *Acta Odontologica Scandinavica*, 31(5), 323-336.

Van Loosen, J., Van Zanten, G. A., Howard, C.V., Verwoerd-Verhoef, H. L., Van, D. V., and Verwoerd, C. D. (1996). Growth characteristics of the human nasal septum. *Rhinology*, 34(2), 78–82.

Wealthall, R. J., & Herring, S. W. (2006). Endochondral ossification of the mouse nasal septum. *The Anatomical Record*, 288(11), 1163-1172.

Weidenreich, F. (1941). The brain and its rôle in the phylogenetic transformation of the human skull. *Transactions of the American Philosophical Society*, 31(5), 328–442.

FIGURE LEGENDS

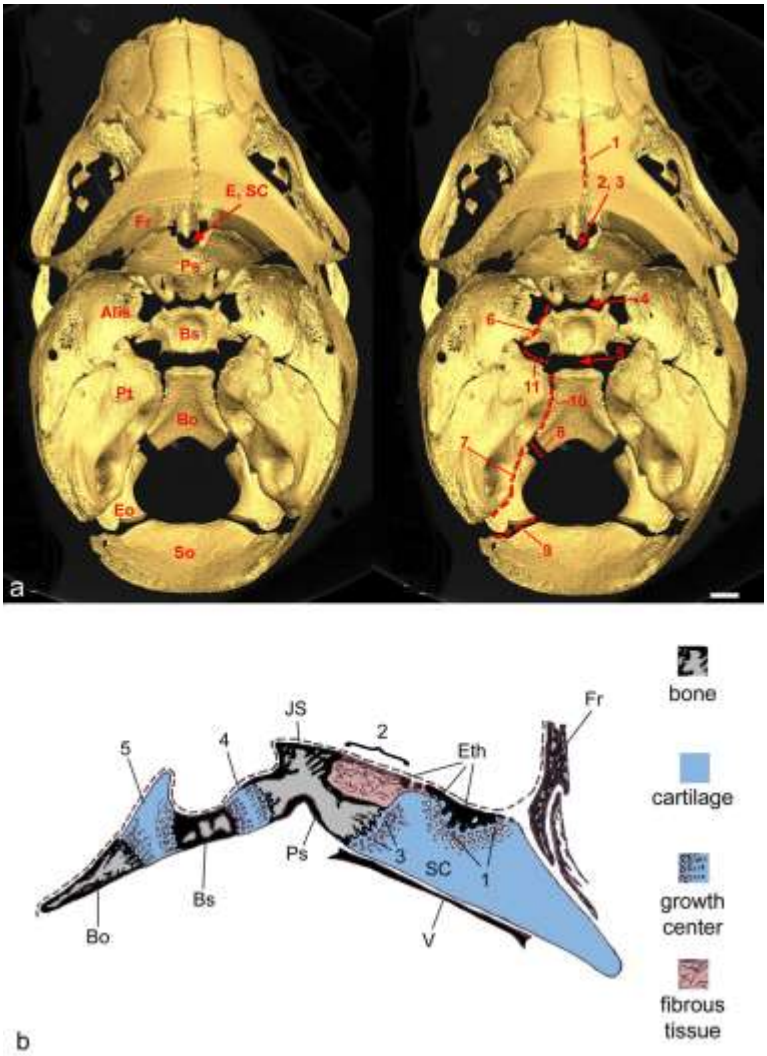

Figure 1: Articulations of basicranial and selected midfacial bones at or near birth. a) A late fetal specimen of *Otolemur crassicaudatus,* viewed from a dorsal perspective, revealing articulations among chondrocranial bones (left side with bone names indicated; right side with bony articulations indicated and numbered per Table 1). Within the anterior cranial fossa there are midline joints between the presphenoid (Ps), ethmoid (E), and sepatal cartilage (SC). More caudally, midline bascranial joints intervene between Ps and the basisphenoid (Bs) and between Bs and the basioccipital (Bo). In the middle cranial fossa, there is are bilateral articulations between the Bs and alisphenoid (Alis). The petrous temporal (Pt) articulates with the Bs at its anteriomedial apex. In the posterior cranial fossa, the Pt articulates with the Bo and exoccipital (Eo). Eo articulates with both the Bo and supraoccipital (So). b) Schematic of mid-sagittal plane histological section of newborn catarrhine (based in part on *Macaca mulatta* and *Papio anubis*). This view reveals that the sphenoid has a complex anterior association with midfacial elements. The presphenoseptal synchondrosis (3) is a ventral association of the presphenoid and septum.

More dorsally, the orbitosphenoid (at the jugum, JS) articulates with the ethmoid. The histological identity of the articulations are informed by the findings of this study. Growth centers indicated are named following Baume (1968) and Wealthall and Herring (2006). Fr, frontal. Scale: a, 2 mm.

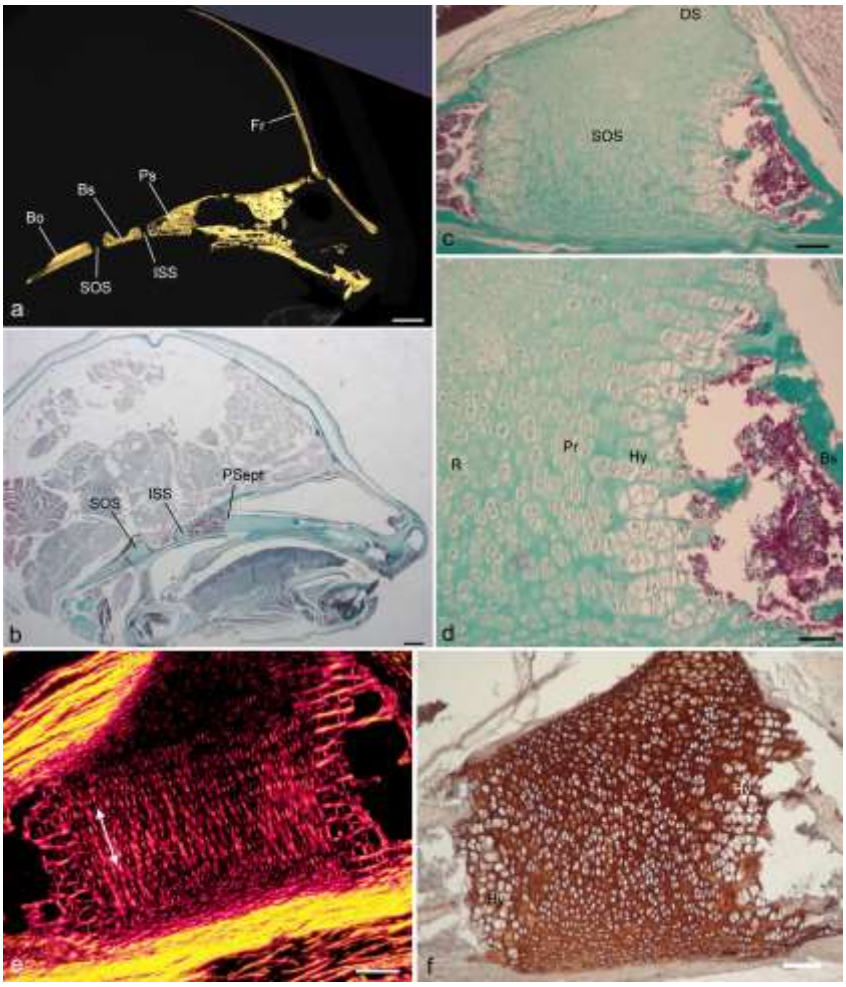

Figure 2: The sphenooccipital synchondrosis (SOS) in *Galago moholi.* a) Midline segment of cranial base in a cranial reconstruction of a newborn *G. moholi*. b) Low magnification view of histology of the same specimen. Each image shows midline bones including the basioccipital (Bo), basisphenoid (Bs) and presphenoid (Ps). Between Bo and Bs is the SOS, a bipolar growth center (c). d) Higher magnification view of SOS showing the resting zone (R), proliferating (Pr) and hypertrophic (Hy) chondrocytes on the cranial side of SOS. e) Picrosirius red preparation viewed using polarized light microscopy reveals most of the SOS (resting and proliferating zones) has a dorsoventral orientation (arrows) of collagen fibers. In the hypertrophic zones, fibers orient longitudinally. f) A section prepared using type II collagen IHC reveals widespread reactivity throughout all zones of SOS. DS, dorsum sellae; Fr, frontal bone; ISS, intrasphenoidal

synchondrosis. PSept, presphenoseptal synchondrosis. Scale bars: a, 1.5 mm; b, 1, mm; c, e, f, 100 µm; d, 50 µm.

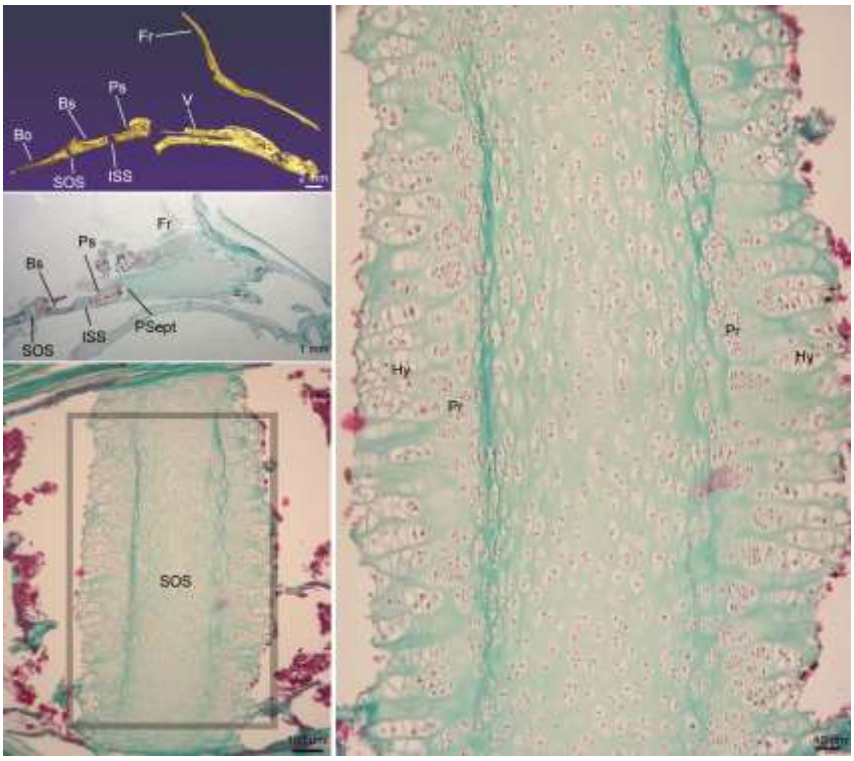

Figure 3: The sphenooccipital synchondrosis (SOS) in *Varecia variegata*. a) Midline segment of cranial base in a cranium reconstruction of a newborn *V. variegata*. b) Low magnification view of histology of the same specimen. Each image shows midline bones including the basioccipital (Bo), basisphenoid (Bs) and presphenoid (Ps). A distinction of *Varecia* spp. is the complete ossification of the dorsum sellae (a,b), which remains cartilaginous in other newborn primates. Between Bo and Bs is the SOS, a bipolar growth center (c). d) Higher magnification view of SOS showing the proliferating (Pr) and hypertrophic (Hy) chondrocytes on both sides of SOS. Fr, frontal bone; R, resting zone V, vomer. Scale bars: a, 2 mm; b, 1, mm; c; 100 µm; d, 40 µm.

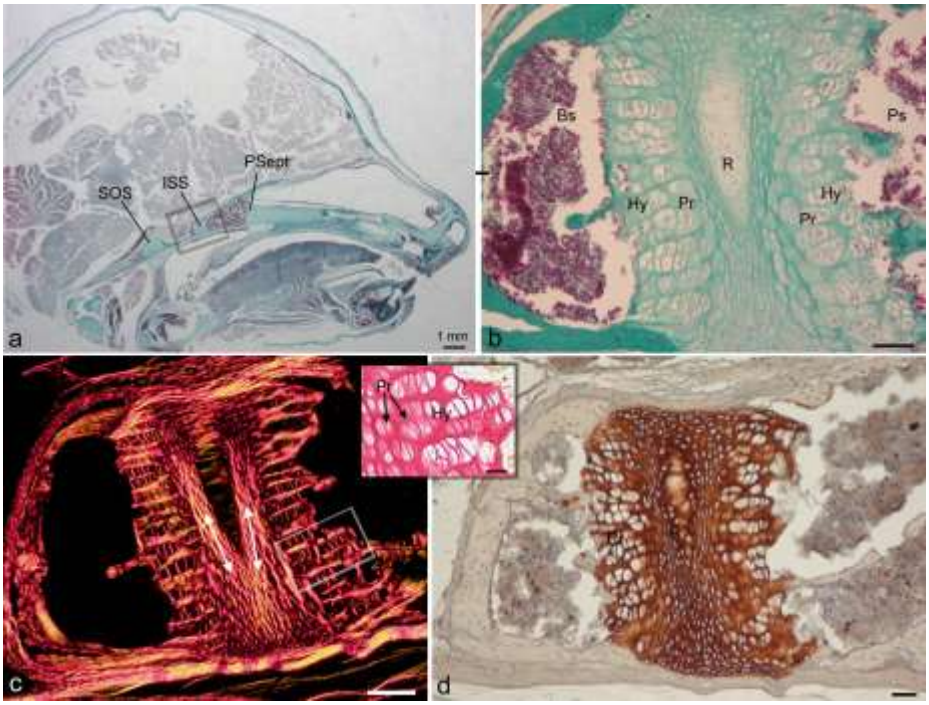

Figure 4: The intrasphenoidal synchondrosis (ISS) in *Galago moholi.* a) Midline section of a newborn *G. moholi.* Midline bones including the basioccipital (Bo), basisphenoid (Bs) and presphenoid (Ps) are indicated. b) Between Bs and Ps is the intrasphenoidal synchondrosis (ISS), a bipolar growth center with a central resting zone (R), and two zones of proliferating (Pr) and hypertrophic (Hy) chondrocytes. c) Picrosirius red preparation viewed using polarized light microscopy reveals most of the ISS (proliferating and especially resting zones) has a dorsoventral orientation (arrows) of collagen fibers, with some divergence near the midline. Fibers orient longitudinally in the hypertrophic zone, also penetrating the zone of proliferating chondrocytes (compare to inset showing the same section with brightfield illumination, enlarged from white box). Note proliferating chondrocytes in clusters. d) A section prepared using type II collagen IHC reveals widespread reactivity throughout most of the ISS, with some attenuation in the zone of hypertrophic chondrocytes. Fr, frontal bone; SOS, sphenooccipital synchondrosis. PSept, presphenoseptal synchondrosis. Scale bars: a, 1, mm; b; 60 µm; c, 100 µm; d, 50 µm; inset 20 µm.

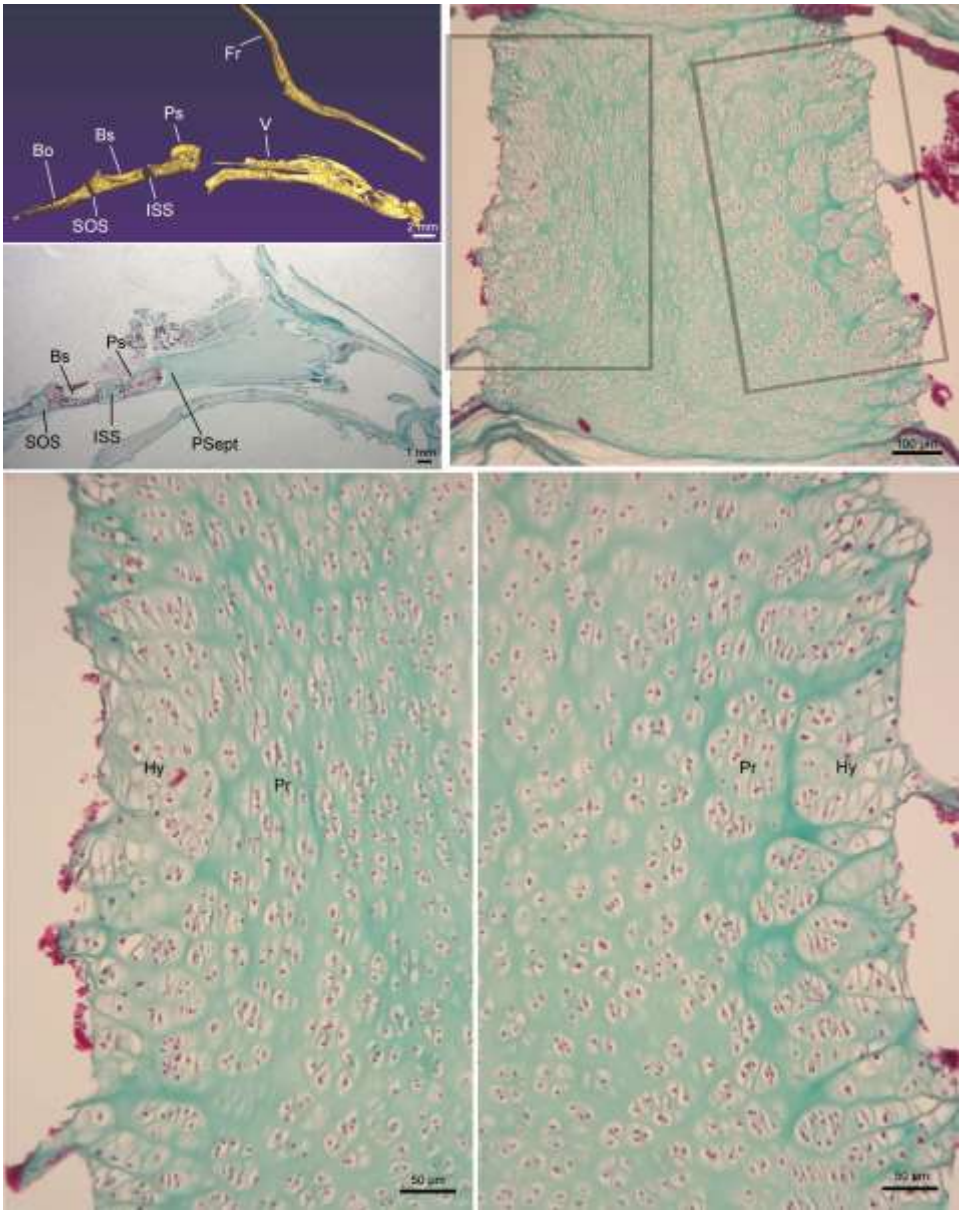

Figure 5: The intersphenoidal synchondrosis (ISS) in *Varecia variegata*. a) Midline segment of cranial base in a cranium reconstruction of a newborn *V. variegata*. b) Low magnification view of histology of the same specimen. Each image shows midline bones including the basioccipital (Bo), basisphenoid (Bs) and presphenoid (Ps). Between Bs and Ps is the ISS, a bipolar growth center (c). d) Higher magnification views of ISS (from boxed areas in c) showing the proliferating (Pr) and hypertrophic (Hy) chondrocytes on both sides of ISS. Scale bars: a, 2 mm; b, 1, mm; c; 100 µm; d, e, 50 µm.

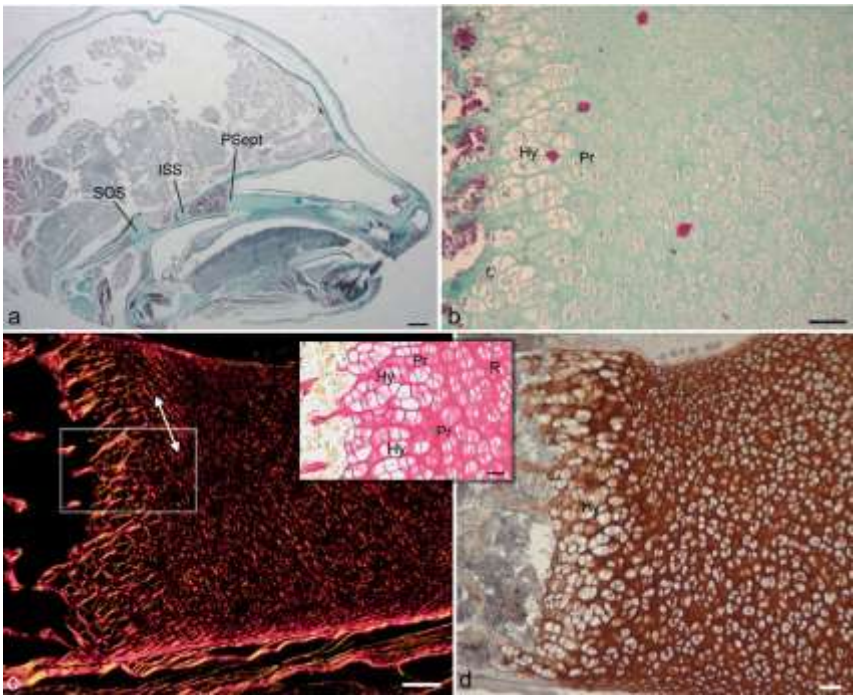

Figure 6: The presphenoseptal synchondrosis (PSept) in *Galago moholi.* a) Midline section of the cranial base in a newborn *G. moholi*, note the midline bones including the basioccipital (Bo), basisphenoid (Bs) and presphenoid (Ps). b) Between Ps and the septal cartilage is the PSept, a unipolar growth center, with the proliferating (Pr) and hypertrophic (Hy) chondrocytes. c) Picrosirius red preparation viewed using polarized light microscopy reveals most of the PSept (resting and proliferating zones) has a latticework organization of fibers with some regions having a preponderance of dorsoventral (arrows) collagen fibers. In the hypertrophic zones, fibers orient longitudinally. The inset is an enlargement of the white boxed area, showing the position of cell zones. d) A section prepared using type II collagen IHC reveals widespread reactivity throughout most of the PSept, but less reactivity in the zone of hypertrophic chondrocytes. Fr, frontal bone; ISS, intrasphenoidal synchondrosis; SOS, sphenooccipital synchondrosis. Scale bars, a, 1 mm; b, 60 µm ; c, 100 µm; d, 200 µm; f, 100 µm.

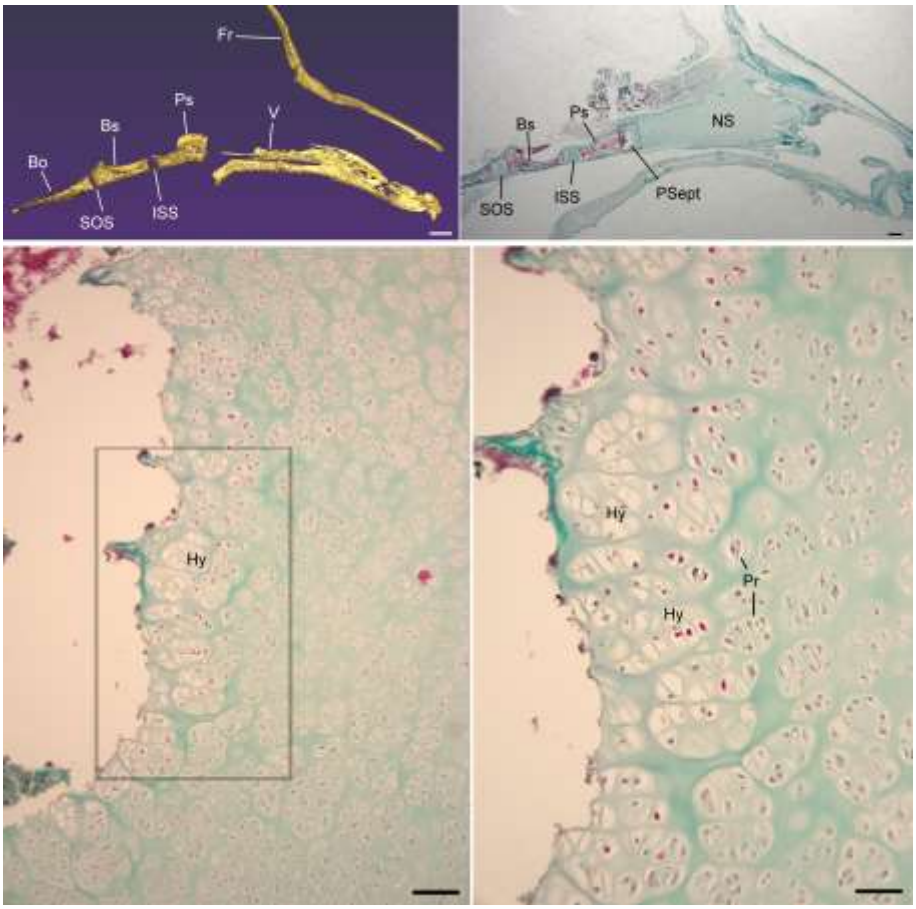

Figure 7. The presphenoseptal synchondrosis (PSept) in *Varecia variegata*. a) Midline segment of cranial base in a cranium reconstruction of a newborn *V. variegata*. b) Low magnification view of histology of the same specimen. Each image shows midline bones including the basioccipital (Bo), basisphenoid (Bs) and presphenoid (Ps). Between Ps and the septal cartilage is the PSept, a unipolar growth center (c). d) Higher magnification view (enlargement of the boxed area in c) of PSept showing the proliferating (Pr) and hypertrophic (Hy) chondrocytes. Scale bars: a, 2 mm; b, 1, mm; c; 100 µm; d, 50 µm.

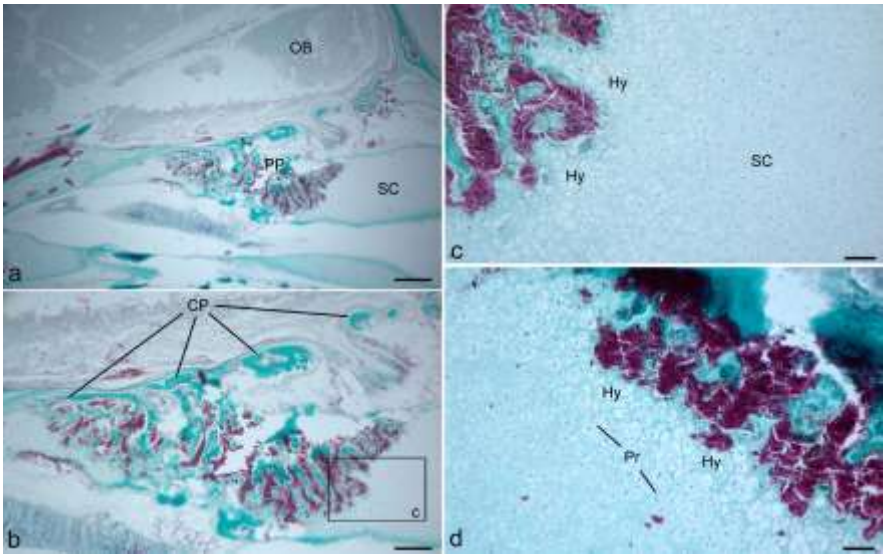

Figure 8: The anterior cranial fossa of *Galago moholi* at birth. a) The ethmoseptal synchondrosis (ESept) radiates in a 180 degree arc within the ossifying perpendicular plate (PP) of the ethmoid. b) Ossified portions of the cribriform plate (CP) are also transected, and border the PP on its lateral sides. c) Higher magnification view (from boxed region in b) showing rows of hypertrophic chondrocytes (Hy) located wherever the PP meets the septal cartilage (SC). d) an adjacent section showing the posterior side of ESept, where hypertrophic chondrocytes are visible, and proliferating chondrocytes (Pr) are sparsely distributed. Scale bars: a, 0.5 mm; b, 250 µm; c, d, 50 µm.

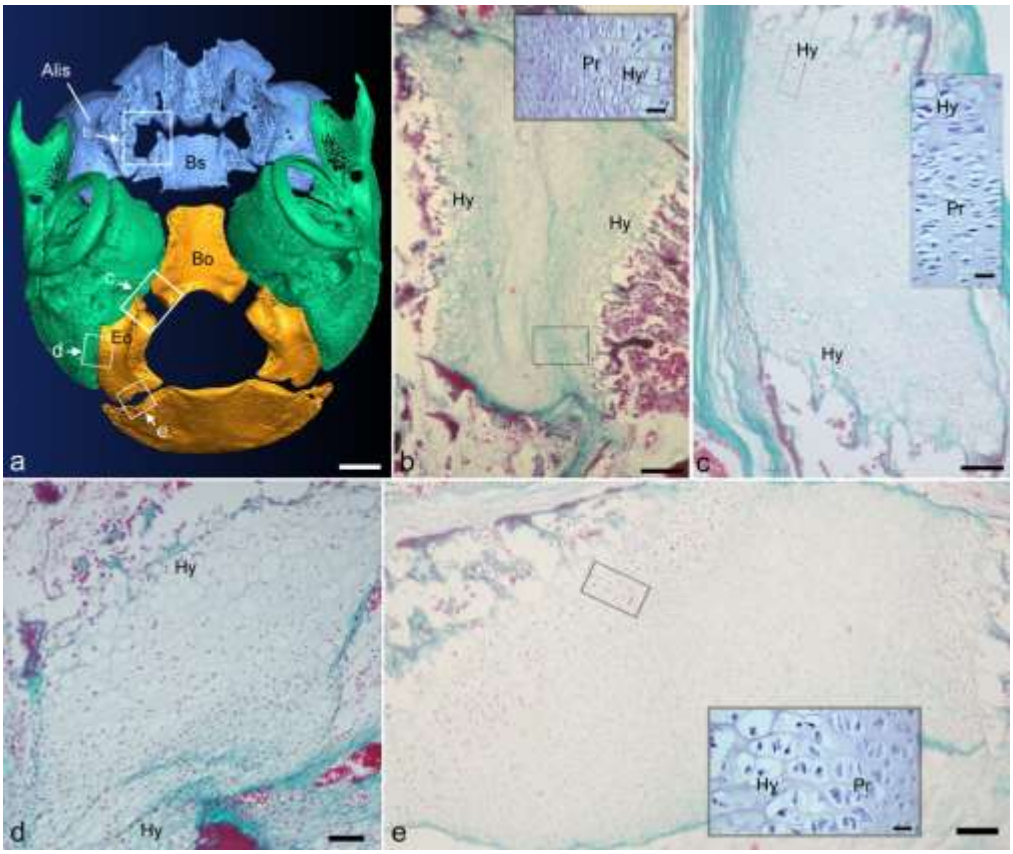

Figure 9: Basilar view of the skull base in a late fetal *Otolemur crassicaudatus*, revealing the sites of bilateral synchondroses found between ossified part of the sphenoid bone (blue), between ossified parts of the occipital bone (orange) and between the occipital and temporal (green) bones. Boxed sites in (a) correspond to histology at the same site in a horizontal plane, including: b) the alibasisphenoidal synchondrosis; c) the anterior intraoccipital synchondrosis; d) the jugular synchondrosis; and e) the posterior intraoccipital synchondrosis. In each synchondrosis, the lightly staining region closest to bone reveals hypertrophic chondrocyte zone (Hy). In most of these synchondroses, a higher magnification (inset) reveals well-organized proliferating (Pr) and hypertrophic chondrocyte zones. In the jugular synchondrosis proliferating zones were indistinct. Alis, alisphenoid; Bo, basioccipital; Bs, basisphenoid; Eo, exoccipital. Scale bars: a, 2 mm; b, c, e, 100 µm; d, 50 µm; all insets, 20 µm.

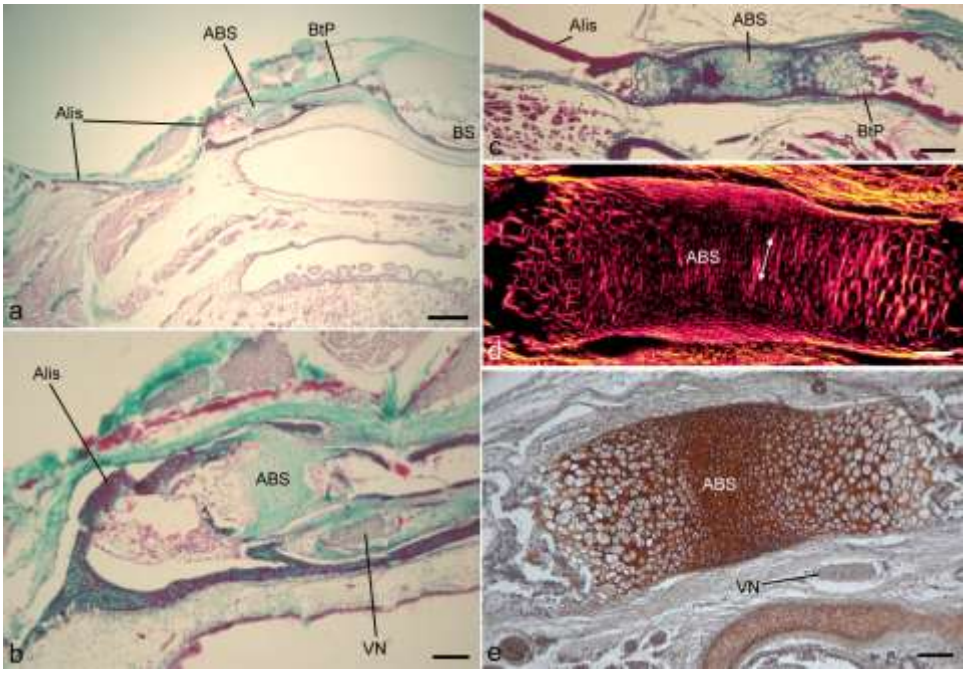

Figure 10: The alibasisphenoidal synchondrosis (ABS) in late fetal *Eulemur collaris* (a, b), newborn *Galago moholi* (c), and late fetal *Otolemur crassicaudatus* (d, e). The ABS connects the basitrabecular process (BtP) of the basisphenoid to the alisphenoid (Alis). a, b) Only a late fetal *Eulemur* specimen still retained cartilage at the ABS, a small nodular mass (b). Note the Vidian nerve (VN) passing inferior to the ABS and BtP. All late fetal and newborn galagids possess an ABS that is flattened and oriented within a horizontal plane (c-e). In the coronal plane, the ABS has the appearance of a bipolar growth centers. Type II collagen fibers are indicated by picrosirius red (d) and immunohistochemical (e) preparations. Fibers in the resting and proliferating zones run dorsoventrally (d). Scale bars, a, 1mm; b-e, 100 µm.

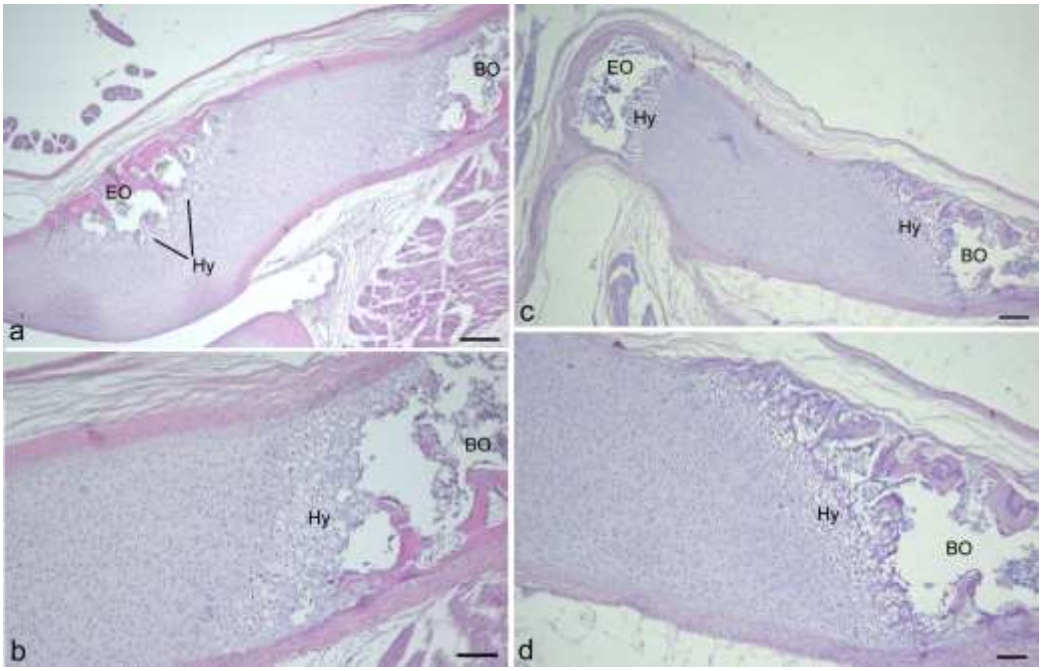

Figure 11: Sagittal (a,b) and coronal plane sections (c,d) of the anterior intraoccipital synchondrosis in late fetal *Eulemur collaris*. The hypertrophic (Hy) zone of chondrocytes stains slightly more lightly than the remainder of the matrix. With this in mind, note the complex contours of growth centers at this joint. In a sagittal plane the exoccipital (Eo) has a radial arc of expansion, reflective of the shape of the occipital condyle (a). Anteriorly (b), the hypertrophic zone is oriented for longitudinal growth at the interface with the basioccipital (Bo). However, examination of the contralateral anterior intraoccipital synchondrosis in the coronal plane (c,d) suggests a mediolateral orientation of growth, indicating a similar overall pattern as in *Otolemur* (see Figs. 8a, c). Scale bars, a, 200 µm; b, 100 µm.; c, 150 µm; d, 75 µm.

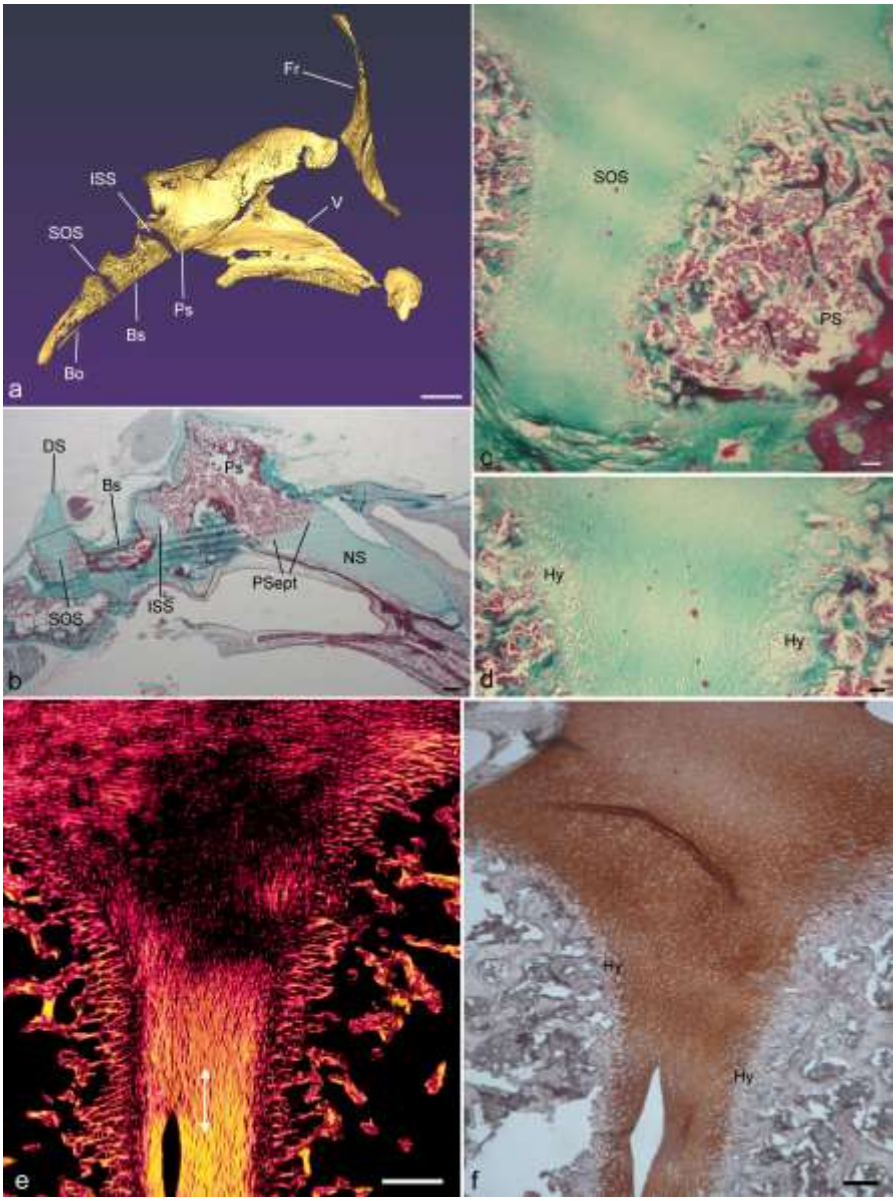

Figure 12: The sphenooccipital synchondrosis (SOS) in *Macaca mulatta.* a) Midline segment of cranial base in a cranium reconstruction of a newborn *M. mulatta*. b) Low magnification view of histology of the same specimen. Each image shows midline bones including the basioccipital (Bo), basisphenoid (Bs) and presphenoid (Ps). Between Bo and Bs is the SOS, a bipolar growth center (c). d) Higher magnification view reveals the more lightly stained zone of hypertrophic (Hy) chondrocytes on both sides of SOS. e) Picrosirius red preparation viewed using polarized light microscopy reveals most of the SOS (resting and proliferating zones) has a dorsoventral orientation (arrowed line) of collagen fibers. In the hypertrophic zones, fibers orient longitudinally. f) A section prepared using type II collagen IHC reveals widespread reactivity throughout all zones of SOS. DS, dorsum sellae; Fr, frontal bone; ISS, intrasphenoidal synchondrosis. PSept, presphenoseptal synchondrosis; V, vomer. Scale bars, a, 4 mm; b, 1 mm; c, 100 µm ; d, 50 µm; e, 200 µm; f, 100 µm.

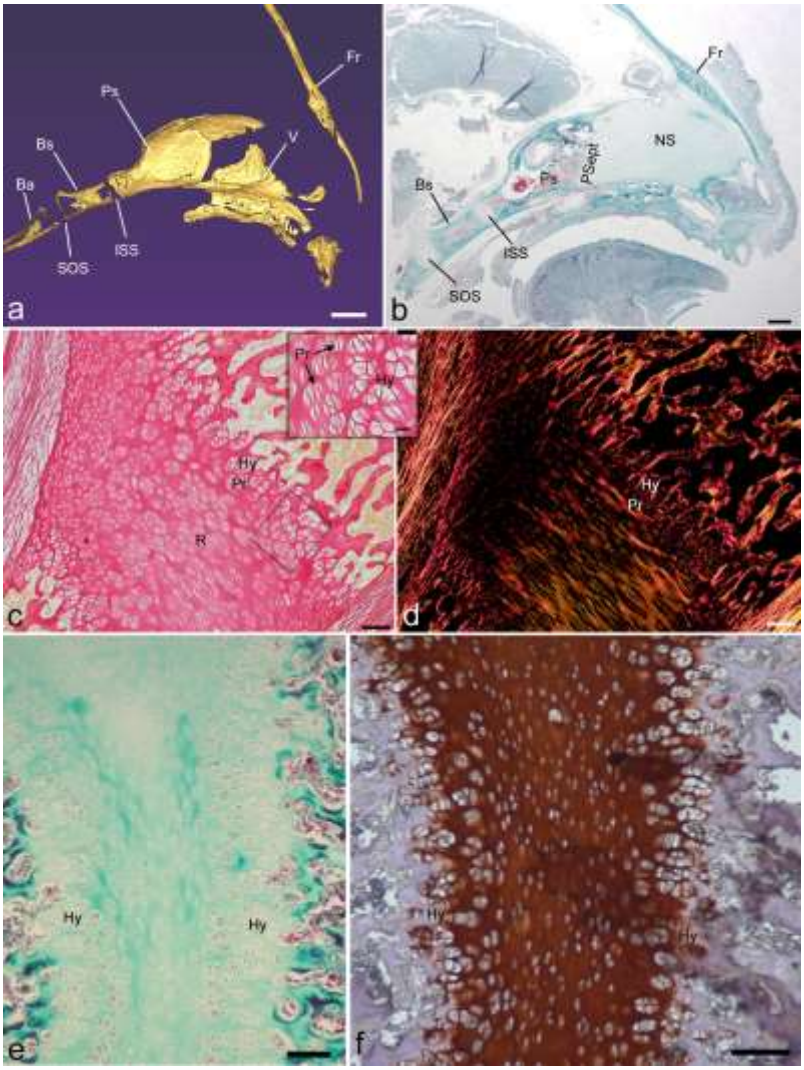

Figure 13: The sphenooccipital synchondrosis (SOS) in a newborn *Saguinus oedipus.* a) Midline segment of the cranial base in a cranium reconstruction. The midline bones including the basioccipital (Bo), basisphenoid (Bs) and presphenoid (Ps) are shown in sagittal perspective. b) Sagittal histological section of the same specimen. c) Between Bo and Bs is the SOS, a bipolar growth center, shown with picrosirius red staining. The inset shows enlarged view of hypertrophic (Hy) and proliferating (Pr) chondrocytes, the latter organized into small columns. d) The same preparation viewed using polarized light microscopy reveals most of the SOS (resting and proliferating zones) has a dorsoventral orientation (arrowed line) of collagen fibers. In the hypertrophic zones, fibers orient longitudinally. e, f) Adjacent sections of the SOS in newborn *Saimiri boliviensis,* prepared using Gomori trichrome and type II collagen IHC procedures. The zone of hypertrophic chondrocytes is lightly stained with Gomori trichrome. Type II collagen reactivity is widespread throughout most of the SOS, except the zone of hypertrophic chondrocytes. Fr, frontal bone; ISS, intrasphenoidal synchondrosis; PSept, presphenoseptal synchondrosis; V, vomer. Scale bars, a, 2 mm; b, 1 mm; c-f, 100 µm; inset, 20 µm.

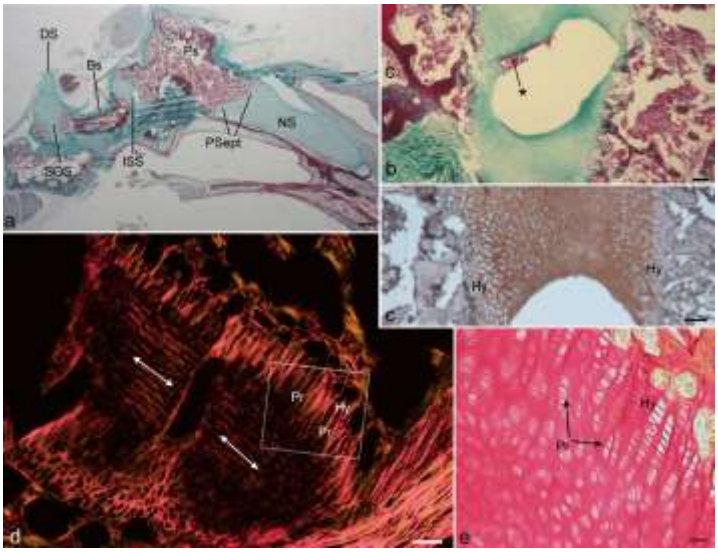

Figure 14: The intrasphenoidal synchondrosis (ISS) in *Macaca mulatta.* a) Between basisphenoid and presphenoid of newborn *M. mulatta* is the ISS. b) In this specimen, ISS had a large central opening within the cartilage, into which a smaller vascular canal (*) communicated. Although the larger space may be artefactually enlarged, we interpret this as a vascularized canal network. c) An nearly adjacent section prepared with type II collagen immunohistochemistry reveals widespread strong reactivity throughout most of the ISS, with weaker reactivity in hypertrophic (Hy) zones. d) A different section of the same specimen viewed using polarized light microscopy reveals most of the ISS (resting and proliferating zones) has a dorsoventral orientation (arrowed line) of collagen fibers. In the hypertrophic zones, fibers orient longitudinally. The inset shows enlarged view of hypertrophic and proliferating (Pr) chondrocytes, the latter organized into columns. a, 1 mm; Scale bars, b-d, 100 µm; e, 20 µm.

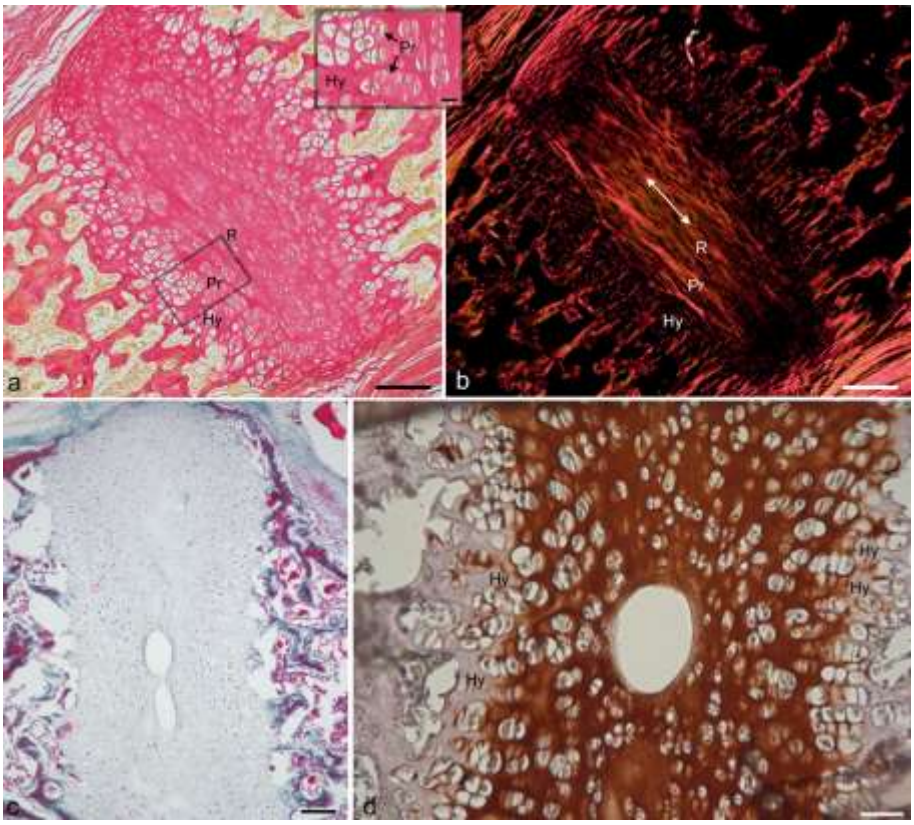

Fig. 15: The intrasphenoidal synchondrosis (ISS) in *Saguinus oedipus* and *Saimiri boliviensis.* a) Between basisphenoid and presphenoid of newborn *Saguinus oedipus* is the ISS, a bipolar growth center, shown with picrosirius red staining. The inset shows enlarged view of hypertrophic (Hy) and proliferating (Pr) chondrocytes, the latter organized into small columns. b) The same preparation viewed using polarized light microscopy reveals most of the ISS (resting and proliferating zones) has a dorsoventral orientation (arrowed line) of collagen fibers. In the hypertrophic zones, fibers orient longitudinally. c, d) Adjacent sections of the ISS in newborn *Saimiri boliviensis,* prepared using Gomori trichrome and type II collagen IHC procedures. Type II collagen reactivity is widespread throughout most of the ISS, except the zone of hypertrophic chondrocytes. Scale bars, a-c, 100 µm; d, 50 µm; inset, 20 µm.

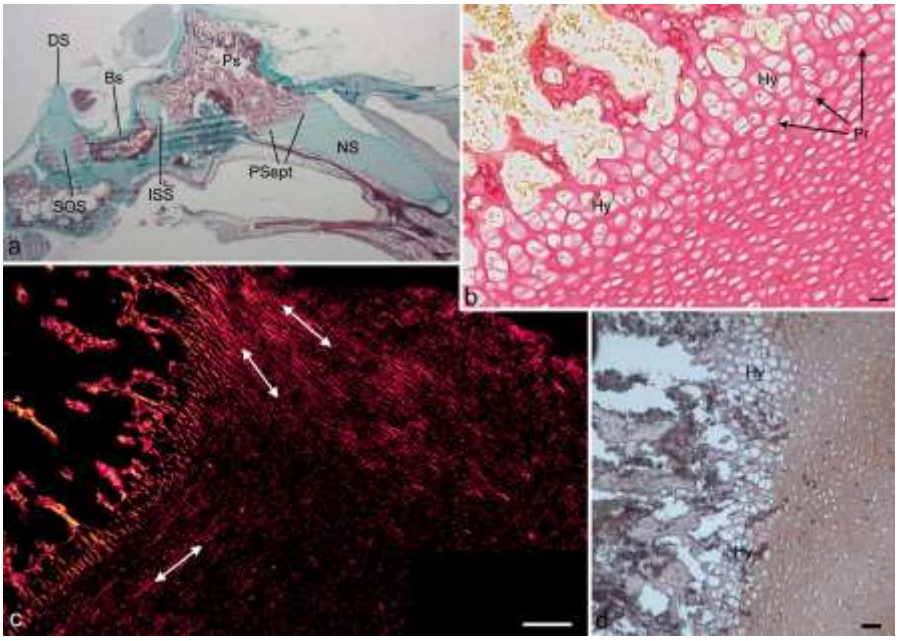

Figure 16: The presphenoseptal synchondrosis (PSept) in *Macaca mulatta.* a) Low magnification view of histology of newborn *M. mulatta*. Midline bones including the basioccipital (Bo), basisphenoid (Bs) and presphenoid (Ps) are indicated. b) Picrosirius red preparation showing hypertrophic (Hy) zone and proliferative (Pr) zone with short columns of chondrocytes. c) The same section as b, viewed using polarized light microscopy. Some groups of organized fibers can be seen running in varied directions. d) A closely adjacent section prepared using type II collagen IHC reveals high reactivity throughout most of PSept, with an attenuated signal in the zone of hypertrophic chondrocytes. SOS, sphenooccipital synchondrosis. ISS, intrasphenoidal synchondrosis. Scale bars, a, 1 mm; b, 20 µm ; c, 200 µm; d, 50 µm.

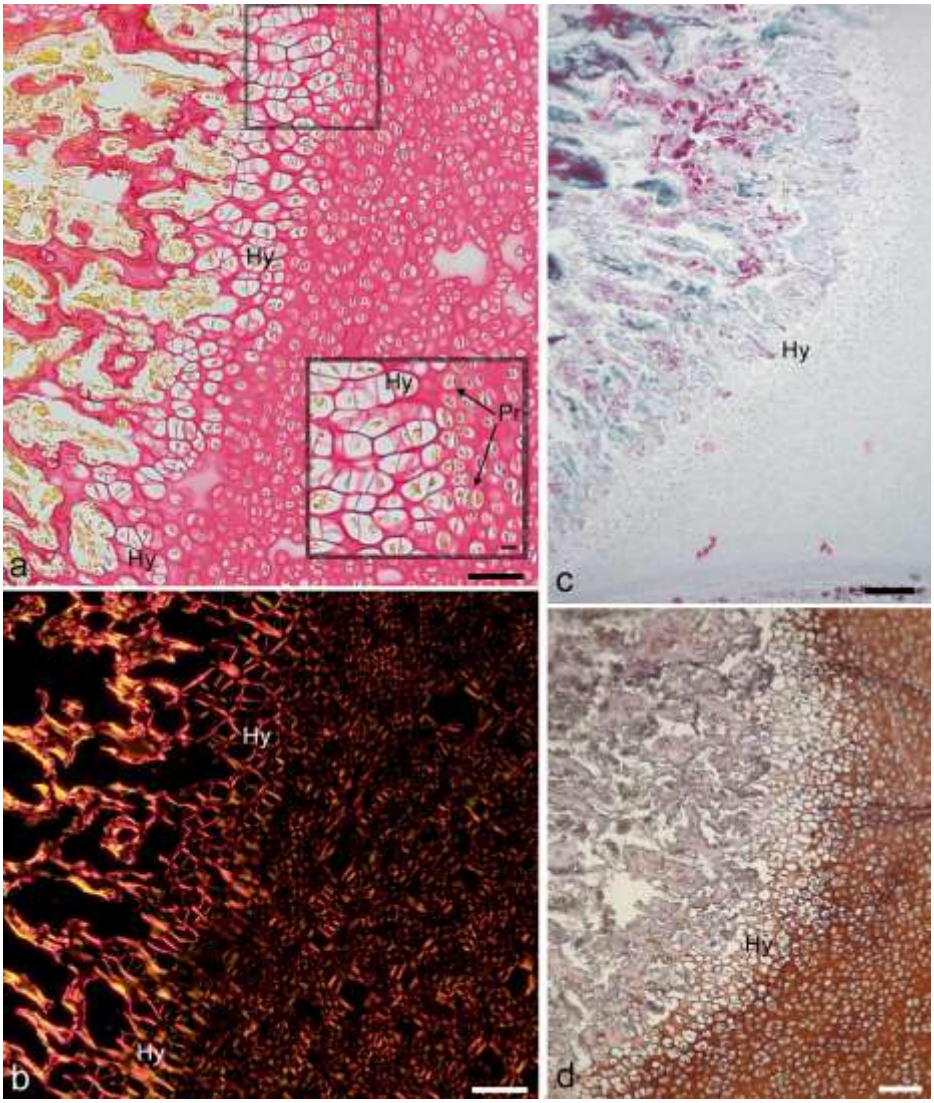

Figure 17: The presphenoseptal synchondrosis (PSept) in *Saguinus oedipus* and *Saimiri boliviensis.* a) Between presphenoid and septal cartilage of *Saguinus oedipus* is the PSept, a unipolar growth center, shown with picrosirius red staining. The inset shows enlarged view of hypertrophic (Hy) and proliferating (Pr) chondrocytes, the latter organized into small clusters of two to three chondrocytes. b) The same preparation viewed using polarized light microscopy reveals PSept is supported by a grid like latticework of collagen fibers. c, d) Adjacent sections of the PSept in newborn *Saimiri boliviensis,* prepared using Gomori trichrome and type II collagen IHC procedures. Note the radial shape of PSept, as shown by the lighter-staining zone of hypertrophic chondrocytes (c). Type II collagen reactivity is widespread throughout most of the PSept, except the zone of hypertrophic chondrocytes (d). Scale bars, a-c, 100 µm; d, 200 µm; inset, 20 µm.

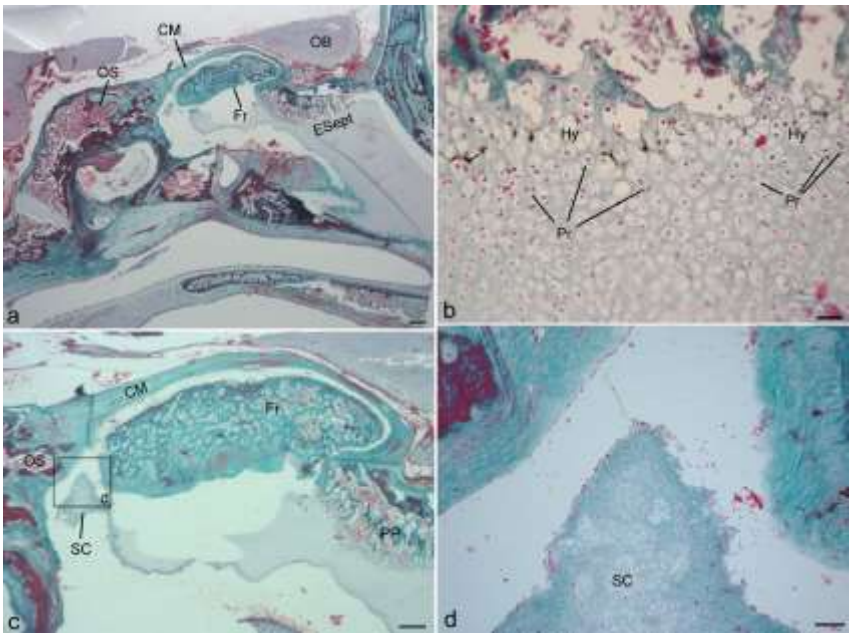

Figure 18: The sphenoethmoidal junction in newborn *Papio anubis*. a) A sagittal section of newborn *P. anubis.* The perpendicular plate (PP) of the ethmoid has commenced ossification, and at its interface with the septal cartilage is the ethmoseptal synchondrosis (ESept). b) ESept has a radial shape (see a) with hypertrophic (Hy) chondrocytes along its margin. Proliferating chondrocytes (Pr) occur in small poorly organized clusters. c) The frontal bone (Fr) projects close to the midline, and the orbitosphenoid (OS) and frontal bones are connected to each other by a collagenous membrane (CM). The septal cartilage (SC) connects the septum to the orbitosphenoid, and is fragmented in this specimen. d) The SC adjacent to the orbitosphenoid lacks the zonal organization of chondrocytes seen at ESept or PSept. Note that the plane is slightly tilted within the sagittal plane, and PSept is visible in a different sectional level. Scale bars, a, c, 1 mm; b, 100 µm ; d, 40 µm.

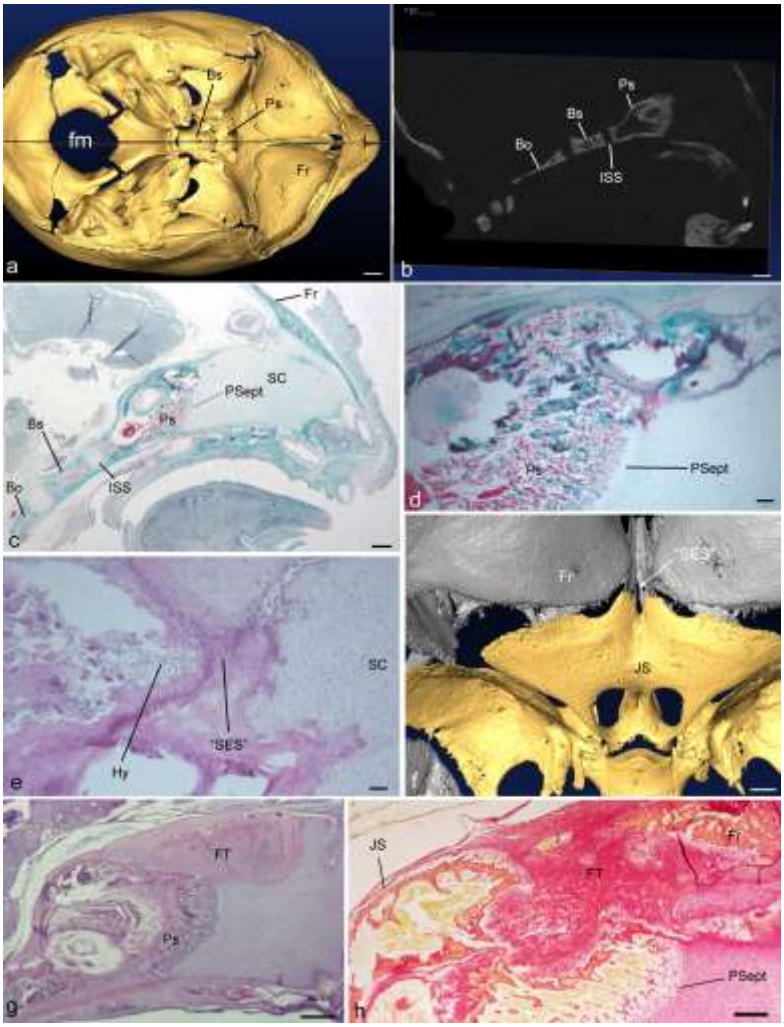

Figure 19: The sphenoethmoidal junction in *Saguinus oedipus* and *Saimiri boliviensis*. a) Basicranium of a newborn *Saguinus oedipus* viewed dorsally, with a line indicating the plane of CT slice shown in (b) revealing a midsagittal cross-section. c) A matching histological section in the same plane, showing a septal cartilage (SC) that is lacking any ossification. The presphenoseptal synchondrosis (PSept) is indicated. d) An enlarged view dorsal to PSept reveals there is no cartilaginous continuity of the SC with the presphenoid. e) An adjacent section reveals the SC is instead united with the presphenoid by fibrous tissue (FT). The site of the sphenoethmoidal synchondrosis ("SES") is indicated. f) Basicranium of newborn *Saimiri boliviensis,* with all but the sphenoid ghosted to emphasize bony articulations in the anterior cranial fossa. Note the frontal bones (Fr) encroach close to the midline, leaving a narrow gap for sphenoethmoidal articulation (i.e., "SES") within the anterior cranial fossa. g-h) Two sections within that narrow interval prepared with hematoxylin and eosin (g, closest to midline) and picrosirius red (h, slightly lateral, with the frontal beginning to articulate). Note only fibrous tissue (FT) exists between the jugum sphenoidale (JS) and the midline septal cartilage at each level. OS, orbitosphenoid. Scale bars, a, b, 1.5 mm; c, 1 mm; d, 200 µm; e, 50 µm; f, g, 1 mm; h, 0.5 mm.

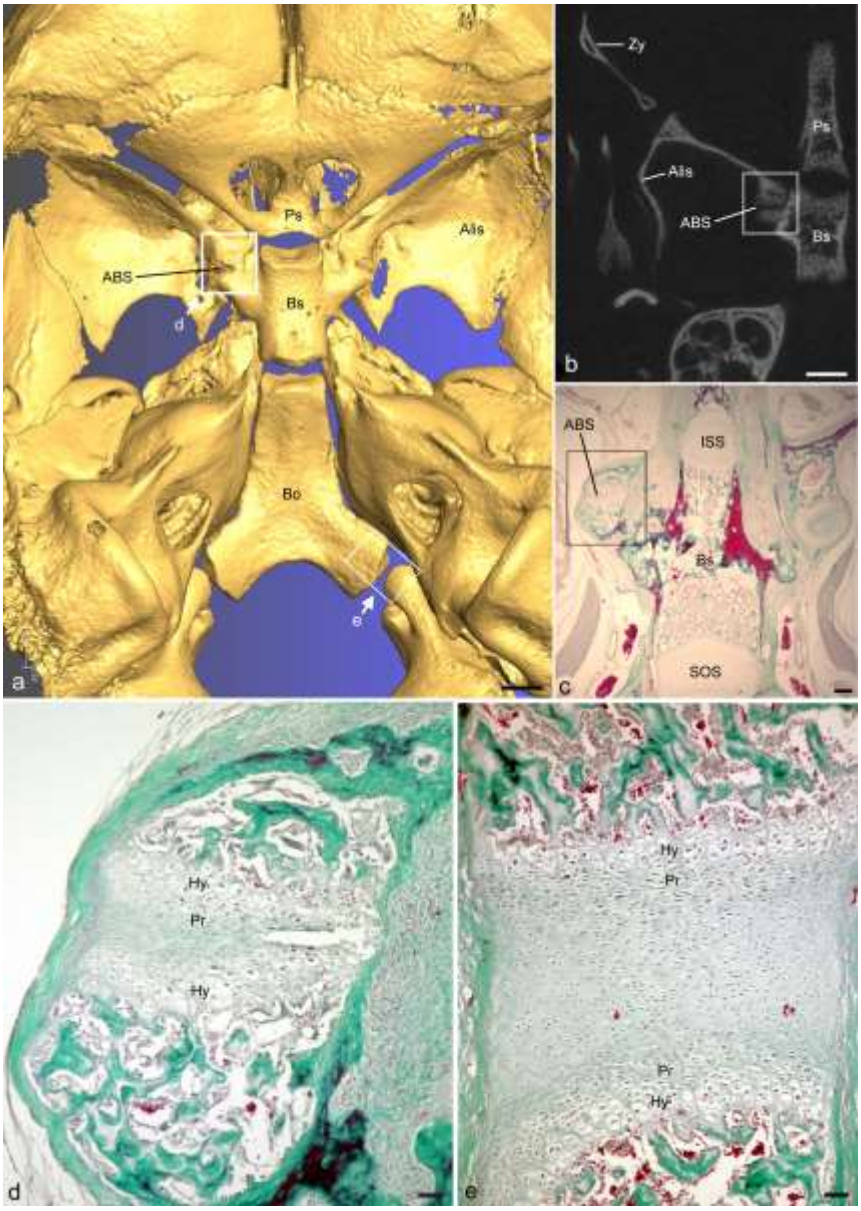

Figure 20: Two bilateral synchondroses in *Callithrix jacchus.* a) Dorsal view of the basicranium in a newborn *C. jacchus*. b) Horizontal CT slice of the same specimen at the level of two bilateral synchondroses. The alibasisphenoidal synchondrosis (ABS) is identifiable as a gap between the basitrabecular process of the basisphenoid (BS) and the most basal part of the alisphenoid (in boxed area of a, b, and c). c) Histological section of the same specimen in a similar plane. The box indicates the site of ABS. d) enlarged from box in (c), showing the ABS is oriented anteroposteriorly, with hypertrophic chondrocytes (Hy) at both sides, and small clusters of proliferating (Pr) chondrocytes seen anteriorly. e) Enlarged from box in (a), the anterior intraoccipital synchondrosis is oriented anteromedially and organized for longitudinal growth in that direction. Scale bars, a, b, 1 mm; c, 200 µm; d, 50 µm; e, 100 µm.

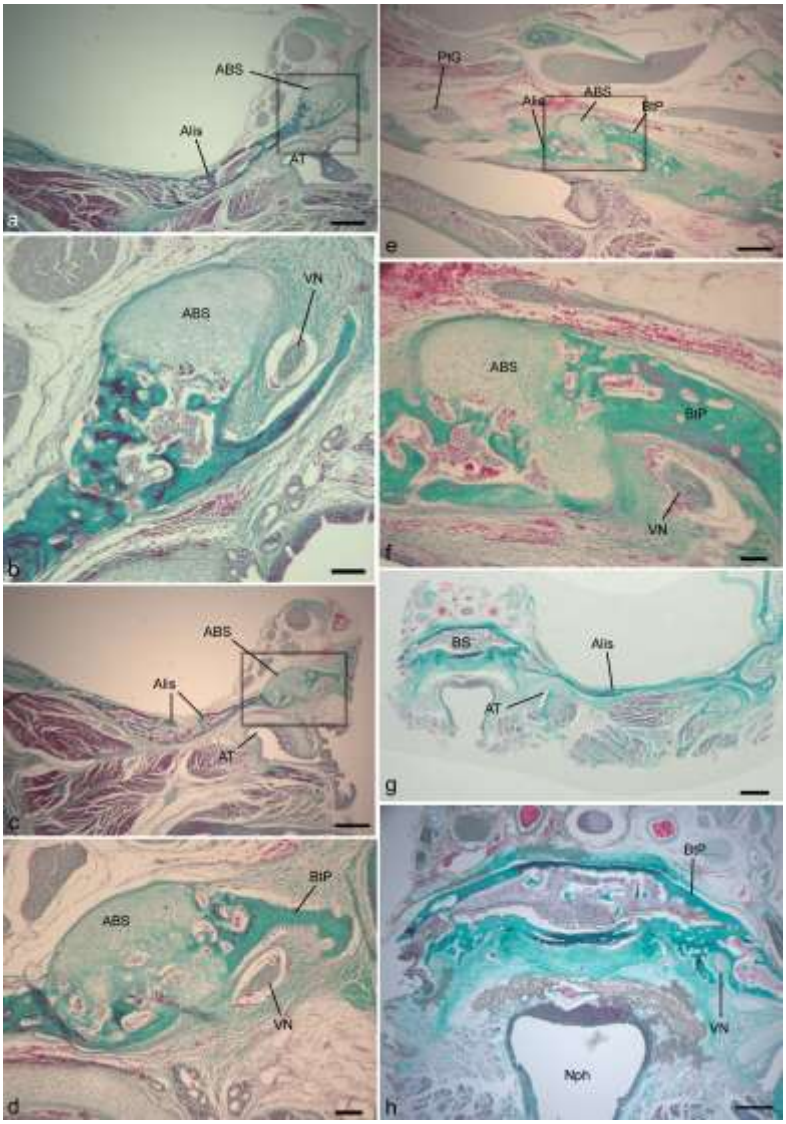

Figure 21: Coronal sections of the alibasisphenoidal synchondroses (ABS) in newborn *Saguinus oedipus* (a-f) and *Saimiri boliviensis* (g, h). The ABS shown where it connects anteriorly to the alisphenoid (Alis: a, enlarged in b) and posteriorly where it connects to the basitrabecular process (BtP: c, enlarged in d) of the basisphenoid (Bs). The Vidian nerve approaches the sphenoid ventral to the basitrabecular process (d) and departs anteriorly on its way to the pterygopalatine fossa (b). e) The contralateral side of the same specimen, sectioned in sagittal planes (left side = anterior). Anterior to the joint, the pterygopalatine ganglion (PtG) is visible. F) An enlarged view reveals that, as in *Callithrix,* the ABS orientation has an anterior component. In newborn *Saimiri boliviensis* (g, h) the ABS is completely fused, but its approximate location is indicated by the Vidian nerve (h). AT, auditory tube; Nph, nasopharynx The Scale bars, a, c, e, h, 0.5 mm; b, d, f, 100 µm; g, 1 mm.

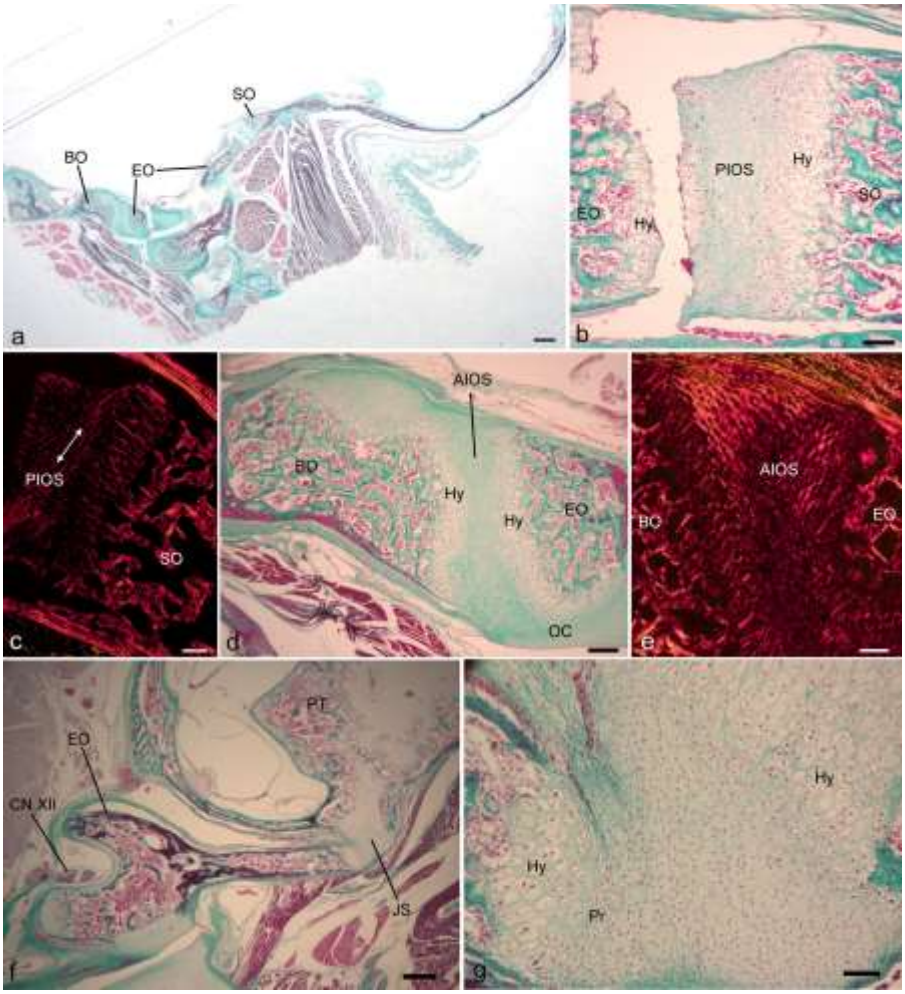

Figure 22: Synchondroses of the posterior cranial fossa in *Saimiri boliviensis,* sectioned in a sagittal plane (a-e) and coronal plane (f, g). a) Low magnification view of the posterior cranial fossa in a newborn, revealing the anterior (AIOS) and posterior (PIOS) intraoccipital synchondroses. b) Enlarged view of the PIOS connecting the exoccipital (EO) and supraoccipital (SO). As in other longitudinal growth centers, note the lighter stained zone of hypertrophic (Hy) chondrocytes at both anterior and posterior ends. c) In an adjacent section with picrosirius red stain, note the dorsoventral orientation of collagen in the central region. d) In this enlarged view of the AOIS, hypertrophic (Hy) zones indicate it is also a bipolar growth center, but posteriorly there is radial expansion at the level of the condyle. The fiber orientation is complex (e, picrosirius red), likely owing to an oblique view of the synchondrosis. f) In a small, notably less developed perinatal *Saimiri* the jugular synchondrosis (JS) connects the exoccipital to the petrous temporal (PT) bones. g) The synchondrosis appears relatively broad in this specimen, because it is continuous with unossified parts of the temporal bone. Medially, hypertrophic (Hy) and proliferating (Pr) chondrocyte zones are clearly visible. OC, occipital condyle. Scale bars: a, 1 mm; b, c, e 100 µm; d, 50 µm; f, 0.5 mm; g, 50 µm.

Supplemental figure legends:

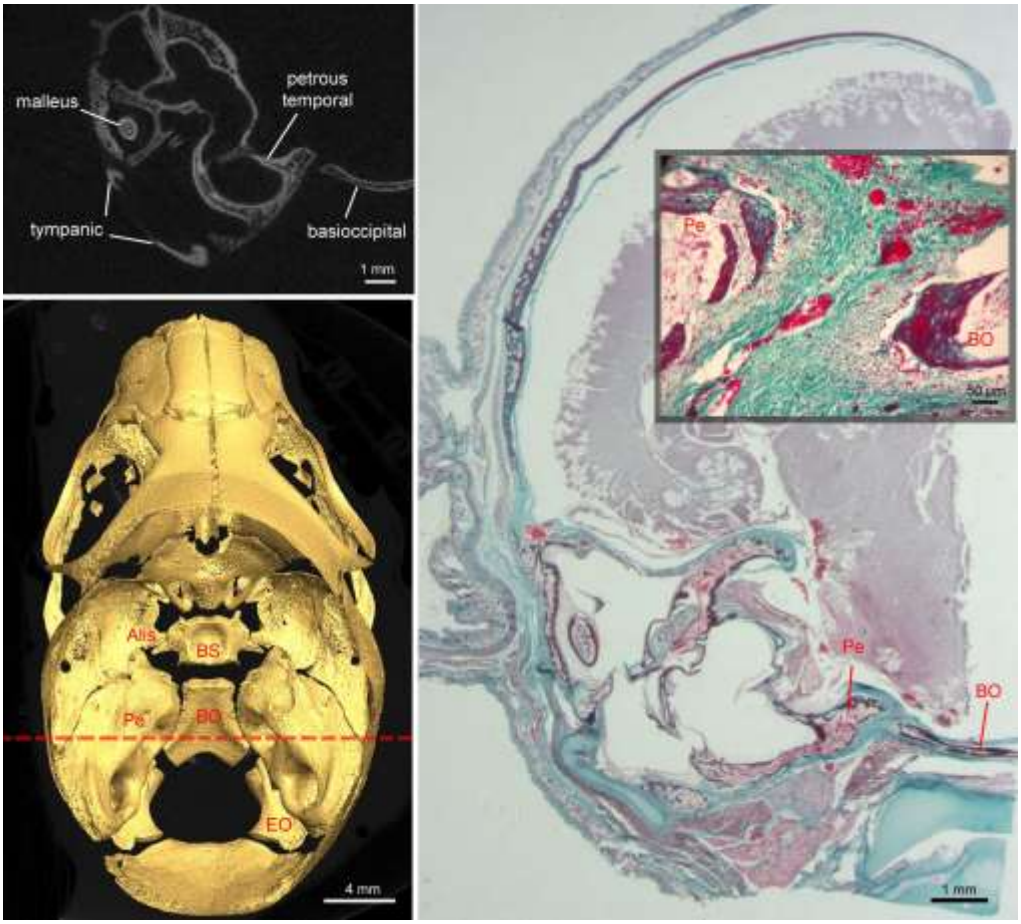

Supplemental Figure 1: Late fetal *Otolemur crassicaudatus*, showing similar micro CT slice levels (top left) and histology (right) through the petrooccipital articulation. The plane is indicated as a dashed line through the basicranium in the lower left image. This joint exists between the petrous temporal (Pe) and basioccipital (BO). The enlarged box on the right reveals only fibrous tissue is found between the bones. Alis, alisphenoid; EO, exoccipital; BS, basisphenoid. Gomori trichrome stain.

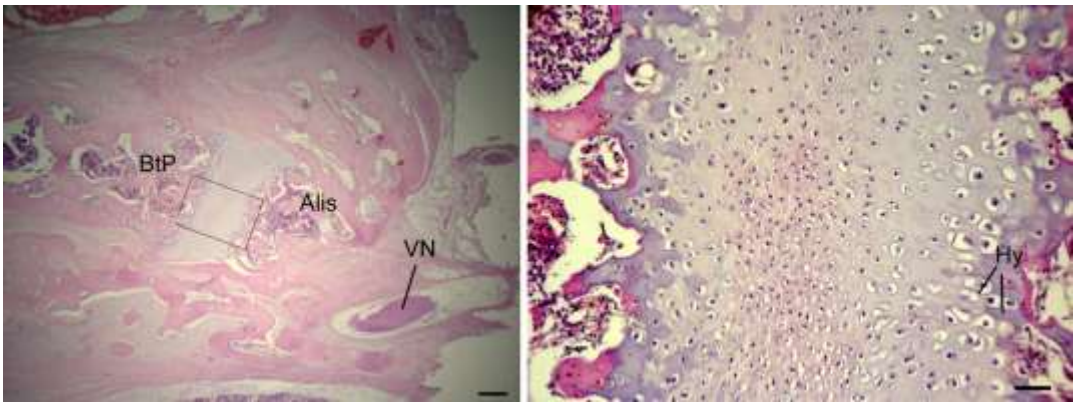

Supplemental Figure 2: The alibasisphenoidal synchondrosis in newborn *Papio anubis*, sectioned in a sagittal plane. Left, the synchondrosis intervenes between the basitrabecular process of the basisphenoid bone (BtP) and the alisphenoid bone (Alis), and orients anteroinferiorly. Note the nearby Vidian nerve. Right, a higher magnification view of the synchondrosis, revealing columns of hypertrophic chondrocytes. Proliferating chondrocytes are not discernable in columns. However, this synchondrosis is most likely cut somewhat obliquely since it also orients anterolaterally; this may obscure columnar organization. Scale bars: a, 300 µm; b, 50 µm.